Linearization and Domain Decomposition Methods for Two-Phase Flow in Porous Media Involving Dynamic Capillarity and Hysteresis

S.B. Lunowa, I.S. Pop, B. Koren

UHasselt Computational Mathematics Preprint
Nr. UP-20-03

Feb. 06, 2020

Linearization and Domain Decomposition Methods for Two-Phase Flow in Porous Media Involving Dynamic Capillarity and Hysteresis*

Stephan Benjamin Lunowa[a,*], Iuliu Sorin Pop[a,b], Barry Koren[c]

[a] *Computational Mathematics, Hasselt University, Agoralaan Gebouw D, 3590 Diepenbeek, Belgium*
[b] *Department of Mathematics, University of Bergen, Norway*
[c] *Department of Mathematics and Computer Science, Eindhoven University of Technology, P.O. Box 513, 5600MB Eindhoven, The Netherlands*

Abstract

We discuss two linearization and domain decomposition methods for mathematical models for two-phase flow in a porous medium. The medium consists of two adjacent regions with possibly different parameterizations. The model accounts for non-equilibrium effects like dynamic capillarity and hysteresis. The θ-scheme is adopted for the temporal discretization of the equations yielding nonlinear time-discrete equations. For these, we propose and analyze two iterative schemes, which combine a stabilized linearization iteration of fixed-point type, the L-scheme, and a non-overlapping domain decomposition method. First, we prove the existence of unique solutions to the problems defining the linear iterations. Then, we give the rigorous convergence proof for both iterative schemes towards the solution of the time-discrete equations.

The developed schemes are independent of the spatial discretization or the mesh and avoid the use of derivatives as in Newton based iterations. Their convergence holds independently of the initial guess, and under mild constraints on the time step. The numerical examples confirm the theoretical results and demonstrate the robustness of the schemes. In particular, the second scheme is well suited for models incorporating hysteresis. Therefore, the schemes can be easily implemented for realistic applications.

Keywords: Linearization, domain decomposition, two-phase flow in porous media, dynamic capillarity, hysteresis
2010 MSC: 65M55, 35K55, 76S05

*This work was supported by the Hasselt University (Project BOF17NI01) and the Research Foundation Flanders (FWO, Project G051418N).

*Corresponding author
Email addresses: stephan.lunowa@uhasselt.be (Stephan Benjamin Lunowa), sorin.pop@uhasselt.be (Iuliu Sorin Pop), b.koren@tue.nl (Barry Koren)

1. Introduction

Porous media flow has been a research field of ongoing interest for years with prominent applications such as CO_2 storage, groundwater pollution and enhanced oil recovery. Understanding the underlying phenomena is crucial for the prediction of these subsurface processes. But measurements are very expensive, if feasible at all, so that mathematical modeling and simulation are the most important tools to gain further insight. The mathematical models typically consist of coupled nonlinear differential equations, which may degenerate and change type in an a-priori unknown manner, depending on the solution itself. While the complexity increases further when dynamic and hysteretic effects are incorporated, largely varying or even discontinuous physical properties pose additional difficulties. Therefore, there is a huge demand for the mathematical design and analysis of suitable, robust computational methods.

Newton based solvers cannot be applied directly to these problems due to severe constraints on the time step sizes to ensure convergence [1]. A simple fixed-point type iteration, the L-scheme, has been proposed as alternative. The high robustness of this method comes at the price of a slower, only linear convergence. This approach is independent of the spatial discretization. It was combined with the (mixed) finite element method in [2, 3] for Richards' equation with equilibrium capillary pressure and two-phase flow with dynamic capillarity, respectively. This approach was used in [4] as a preconditioner for the Newton method. In [5], the L-scheme was used together with a discontinuous Galerkin method for the two-phase system with dynamic effects, neglecting hysteresis. A multi-point flux approximation finite volume method was applied in [6] for two-phase flow incorporating dynamic capillarity. Whereas the analysis is commonly accomplished assuming Lipschitz continuous parameter functions, it was extended in [7, 8] to Richards' and two-phase equations, involving only Hölder continuous coefficients, such as the often used van Genuchten-Mualem parameterization.

In the situation of layered soil, it seems natural to additionally apply a domain decomposition method to decouple the essentially different layers and thereby speeding up the convergence. Though stemming from 1870 [9], domain decomposition methods became subject to intensive research only 100 years later, starting with [10, 11]. Henceforth, it became used and optimized for a wide range of applications, see e.g. [12–16]. In [17], a non-overlapping domain decomposition method was analyzed for nonlinear convection-diffusion equations in a time-continuous setting. Such methods can be also used after temporal discretization for porous media equations, as proposed in [18, 19] for a simplistic setting, while Richards' equation and the two-phase flow equations were considered in [20, 21], where a-posteriori error estimates and multirate time stepping methods were derived. In [22, 23], the domain decomposition was integrated in the linearization process for both Richards' equation and two-phase flow, and the convergence is proved rigorously.

Here, we propose two linearization and domain decomposition schemes for two-phase flow in block-heterogeneous porous media. The model includes dynamic effects and hysteresis in the capillary pressure formulation. These methods are independent of the concrete space discretization and avoid the use of derivatives as in Newton based iterations. By maintaining the formulation of the equations in physical variables, instead of using the Kirchhoff transformation, these schemes are particularly accessible for di-

rect application in the engineering context. This work generalizes and substantiates the preliminary results reported in [24, 25].

This article is structured in the following way: The two-phase flow model, the notation and the assumptions are introduced in Section 2. In Section 3, the temporal discretization by the implicit θ-scheme is stated. Based on this, the iterative schemes for finding the solutions to the nonlinear semi-discrete equations are derived. The analysis in Section 4 contains proofs for the existence of unique solutions to the problems defining the linear iterations and for the convergence of the iterative solutions. Section 5 addresses the numerical validation of the theoretical results by several examples in two spatial dimensions. Finally, Section 6 completes this work with a discussion and outlook.

2. Mathematical Model of Non-Equilibrium Two-Phase Flow in Porous Media

Let the domain $\Omega \subset \mathbb{R}^d$ for $d \in \mathbb{N}$ with a Lipschitz boundary $\partial\Omega$ and the final time $T > 0$ be fixed. The domain is partitioned into two disjoint subdomains Ω_1 and Ω_2 with Lipschitz boundaries $\partial\Omega_l$ and outer normal vectors ν_l for $l \in \{1, 2\}$, which henceforth denotes the subdomain index. Furthermore, the subdomains are separated by the interface $\Gamma = \Omega \setminus (\Omega_1 \cup \Omega_2)$, assumed to be a $(d-1)$-dimensional manifold (see also Fig. 1). Note that the extension of this and all the following to more than two subdomains is straightforward, see [22, Rem. 3 & Sec. 4.4]. All the following quantities can depend on their position in the domain, but we suppress this dependence for the ease of presentation. In each subdomain Ω_l, the dimensionless formulation

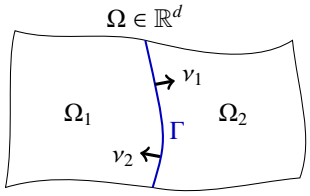

Figure 1: Schematic sketch of a block-heterogeneous domain $\Omega = \Omega_1 \cup \Gamma \cup \Omega_2$ with interface Γ.

for flow of two immiscible, incompressible phases through a stationary, rigid porous medium is governed by the mass balance equations

$$-\phi_l \partial_t s_l + \nabla \cdot \mathbf{u}_{n,l} = q_{n,l} \qquad \text{in } \Omega_l \times (0, T), \tag{2.1}$$

$$\phi_l \partial_t s_l + \nabla \cdot \mathbf{u}_{w,l} = q_{w,l} \qquad \text{in } \Omega_l \times (0, T), \tag{2.2}$$

where $\phi_l \in (0, 1)$ is the medium porosity and s_l is the saturation of the wetting phase (note that in a two-phase system $s_n + s_w = 1$, i.e. only one saturation is necessary). The source rate of the α-phase ($\alpha \in \{n, w\}$) is denoted by $q_{\alpha,l}$. The specific discharge $\mathbf{u}_{\alpha,l}$ of the α-phase incorporates the intrinsic permeability K_l, which is a second rank tensor for anisotropic media, and the relative mobility $\lambda_{\alpha,l}$ due to the extended Darcy law,

$$\mathbf{u}_{\alpha,l} = -\lambda_{\alpha,l}(s_l) K_l \nabla p_{\alpha,l} \qquad \text{in } \Omega_l \times (0, T). \tag{2.3}$$

Here, $p_{\alpha,l}$ denotes the pressure in the α-phase. Note that addition of (2.1) and (2.2) implies that the total discharge $\mathbf{u}_{n,l} + \mathbf{u}_{w,l}$ is divergence free whenever the total source rate $q_{n,l} + q_{w,l}$ vanishes.

At the interface Γ separating the two subdomains, we assume that the normal flux and the pressure of each phase are continuous, i.e. for $\alpha \in \{n, w\}$

$$\mathbf{u}_{\alpha,1} \cdot \nu_1 = -\mathbf{u}_{\alpha,2} \cdot \nu_2, \qquad p_{\alpha,1} = p_{\alpha,2} \qquad \text{on } \Gamma \times (0,T). \tag{2.4}$$

Remark 2.1 (Interface conditions). The continuity of the normal fluxes follows directly from mass conservation. The continuity of the phase pressure is valid, if the phase is present at both sides of the interface. This is not necessarily valid any more for so-called entry-pressure models, when the non-wetting phase is absent at one side of the interface, as shown in [26–28] for standard models and [29] for dynamic capillary pressure. To the best of our knowledge, conditions for entry-pressure models including both, dynamic and hysteretic effects, have not yet been proposed or derived.

Typically, one assumes that the phase-pressure difference $p_n - p_w$ is a function of the wetting saturation, the so-called equilibrium capillary pressure $p_c(s_w)$, which can be obtained by experiments under quasi-equilibrium conditions. But the experimental results reported e.g. in [30–33] are ruled out by this standard model. To deal with this, non-equilibrium models incorporating dynamic effects and hysteresis were studied e.g. in [34–40]. Here, we consider the play-type hysteresis model proposed in [41, 42],

$$p_{n,l} - p_{w,l} \in p_{c,l}(s_l) - \gamma_l \operatorname{sign}(\partial_t s_l) - \tau_l(s_l)\partial_t s_l, \tag{2.5}$$

where the non-negative function τ_l and $\gamma_l \geq 0$ model the effects due to dynamic capillarity and hysteresis, respectively. We refer to [43–46] for a mathematical investigation of saturation overshoots or finger-type profiles. For the following analysis, we use a regularization $\Phi_{\delta,l}$ of the scaled sign function to obtain a single-valued relation and to ensure strict monotonicity. For fixed, small parameter $\delta > 0$ and $l \in \{1, 2\}$, the regularization is given by

$$\Phi_{\delta,l}(\xi) = \begin{cases} \gamma_l \operatorname{sign}(\xi) & \text{if } |\xi| \geq \delta, \\ \gamma_l \frac{\xi}{\delta} & \text{if } |\xi| < \delta. \end{cases}$$

The regularized non-equilibrium capillary pressure condition then becomes

$$p_{n,l} - p_{w,l} = p_{c,l}(s_l) - \Phi_{\delta,l}(\partial_t s_l) - \partial_t T_l(s_l) \qquad \text{in } \Omega_l \times (0,T), \tag{2.6}$$

where T_l denotes the primitive of τ_l.

For uniformly positive τ, the multi-valued equation (2.5) can be solved in $\partial_t s$, as done in [47–49]. This yields a single-valued function $\hat{\Psi}_l$, such that one can rewrite the capillary pressure relation in the inverted form $\partial_t s_l = \hat{\Psi}_l(s_l, p_{n,l} - p_{w,l})$. This formulation has the major advantage that it imposes explicit values for the time derivative of the saturation, and avoids a multi-valued relation like (2.5). Here, we consider the inverse capillary pressure condition only for constant $\tau_l > 0$, which then becomes

$$\partial_t s_l = \Psi_l(p_{n,l} - p_{w,l} - p_{c,l}(s_l)) \qquad \text{in } \Omega_l \times (0,T), \tag{2.7}$$

where

$$\Psi_l(p) = \begin{cases} \frac{-p+\gamma_l}{\tau_l} & \text{if } p \geq \gamma_l, \\ 0 & \text{if } |p| < \gamma_l, \\ \frac{-p-\gamma_l}{\tau_l} & \text{if } p \leq -\gamma_l. \end{cases}$$

A regularization of Ψ_l matching $\Phi_{\delta,l}$ was used in [43, 45, 48, 50] to prove the existence of weak solutions for $\delta \to 0$, and to develop appropriate numerical schemes. Moreover, it is possible to only include hysteresis and no dynamic effects. Then, Ψ_l has to be regularized by including e.g. a small dynamic effect, namely taking $\tau_l = \varepsilon > 0$.

Remark 2.2. Richards' equation models unsaturated flow in porous media [51], based on the simplification that the non-wetting pressure p_n is constant, such that (2.1) can be neglected. Although this paper focuses on the general two-phase flow equations, the results can be directly transferred to Richards' equation.

2.1. Notation

We denote by $L^2(X)$, $H^1(X)$, $H^1_0(X)$ and $H^{\mathrm{div}}(X)$ the standard Hilbert spaces on $X \in \{\Omega, \Omega_1, \Omega_2\}$. $H^{1/2}(\Gamma)$ consists of all traces of functions in $H^1(\Omega)$. This trace on Γ of $w \in H^1(\Omega)$ is denoted by $w|_\Gamma$. For any function $f \in L^2(\Omega)$, $f_l := f|_{\Omega_l}$ denotes the restriction to Ω_l for $l \in \{1, 2\}$. Vice versa, a pair of functions $(f_1, f_2) \in L^2(\Omega_1) \times L^2(\Omega_2)$ is identified with the natural L^2-extension f on the whole domain Ω. For simplicity, we only consider homogeneous Dirichlet boundary conditions at $\partial\Omega$ for the pressures, so that the following spaces will be used

$$\mathcal{W}_l := \{w \in H^1(\Omega_l) \,:\, w|_{\partial\Omega_l \cap \partial\Omega} \equiv 0\}, \qquad \mathcal{W} := L^2(\Omega) \times [\mathcal{W}_1 \times \mathcal{W}_2]^2.$$

At the expense of additional technical effort, it is possible to extend the results in this article to other types of boundary conditions. Since $\partial\Omega \cap \partial\Omega_l$ is either empty or has positive $(d-1)$-measure, the functions in $\mathcal{W}_l$ vanish on this common part of the boundary. Note that $w \in H^1_0(\Omega)$ is equivalent to $(w_1, w_2) \in \mathcal{W}_1 \times \mathcal{W}_2$ with $w_1|_\Gamma \equiv w_2|_\Gamma$. This is a direct consequence of the trace theorem. For the continuity of the pressure across the interface Γ, we introduce the space

$$\mathcal{V} := L^2(\Omega) \times [H^1_0(\Omega)]^2.$$

Moreover, the space for the interface conditions on Γ is given by

$$H^{1/2}_{00}(\Gamma) := \{w \in H^{1/2}(\Gamma) \,:\, \exists v \in H^1_0(\Omega) \,:\, v|_\Gamma \equiv w\}.$$

It is a Hilbert space as the quotient space $H^1_0(\Omega)/\ker(\cdot|_\Gamma)$, see [52, Prop. 2.3]. The L^2 inner product and norm on $X \in \{\Omega_1, \Omega_2, \Gamma\}$ are denoted by $(\cdot,\cdot)_X$ and $\|\cdot\|_X$. Analogously, $\langle\cdot,\cdot\rangle_\Gamma$ stands for the dual pairing on $H^{1/2}_{00}(\Gamma)$ with $H^{1/2}_{00}(\Gamma)'$ via the Gelfand triple with $L^2(\Gamma)$. Here and in the following, the dual of a Banach space B is denoted by B'.

2.2. Assumptions on the Coefficient Functions

In the following, we summarize all assumptions on the coefficient functions, which are mostly also found in realistic physical systems. Note that we explicitly exclude the degeneration of the equations by requiring positive mobilities λ_α and a Lipschitz continuous equilibrium capillary pressure p_c. In realistic applications, where these assumptions do not hold, one can use a regularization like in [49, 53–56], where the convergence of the solutions of the regularized equations towards the solution of the degenerated equations and the existence of the latter solutions were proved.

Assumption 1. For $l \in \{1, 2\}$ and $\alpha \in \{n, w\}$, assume that

- $K_l : \Omega_l \to \mathbb{R}^{d\times d}$ is symmetric and there exist constants $\underline{K}_l, \overline{K}_l \in \mathbb{R}^+$ such that $\underline{K}_l \|\xi\|^2_{\mathbb{R}^d} \leq \xi^T K_l(x)\xi \leq \overline{K}_l \|\xi\|^2_{\mathbb{R}^d}$ for all $x \in \Omega_l$ and $\xi \in \mathbb{R}^d$,
- $\lambda_{\alpha,l} : \mathbb{R} \to \mathbb{R}^+$, is Lipschitz continuous with Lipschitz constant $L_{\lambda_\alpha,l}$ and there exist $m_{\lambda_\alpha,l}, M_{\lambda_\alpha,l} \in \mathbb{R}^+$ such that $m_{\lambda_\alpha,l} \leq \lambda_{\alpha,l}(s) \leq M_{\lambda_\alpha,l}$ for all $s \in \mathbb{R}$,
- $q_{\alpha,l} : [0, T] \to L^2(\Omega_l)$ is continuous,
- $p_{c,l} : \mathbb{R} \times \Omega_l \to \mathbb{R}$ is strictly monotonically decreasing in the first variable, Lipschitz continuous and constants $m_{p_c,l}, L_{p_c,l} \in \mathbb{R}^+$ exist such that $m_{p_c,l} |r - s| \leq \left|p_{c,l}(r, x) - p_{c,l}(s, x)\right| \leq L_{p_c,l} |r - s|$ for all $r, s \in \mathbb{R}$ and $x \in \Omega_l$,
- $\tau_l : \mathbb{R} \to \mathbb{R}^+$ is measurable and there exist constants $m_{T,l}, L_{T,l} \in \mathbb{R}^+$ such that $m_{T,l} < \tau_l(s) < L_{T,l}$ for all $s \in \mathbb{R}$; Its primitive $T_l : \mathbb{R} \to \mathbb{R}$ is bi-Lipschitz continuous and strictly monotonically increasing,
- $\gamma_l : \Omega_l \to [0, \infty)$ is Lipschitz continuous and bounded by a constant $M_{\gamma,l} \in \mathbb{R}^+$.

Remark 2.3. The extension of $\lambda_{\alpha,l}$, $p_{c,l}$ and τ_l to any value $s \in \mathbb{R}$ is necessary because the non-degenerated, non-equilibrium model does not satisfy a maximum principle due to possible overshoots. However, the solutions of the degenerated model remain (essentially) bounded, see [54, 55]. Nevertheless, these extensions can be constructed naturally, only assuming Lipschitz continuity on $[0, 1]$.

Remark 2.4. By Assumption 1, $\Phi_{\delta,l} : \mathbb{R} \times \Omega_l \to \mathbb{R}$ is monotonically increasing in the first variable and Lipschitz continuous with Lipschitz constant $L_{\Phi_\delta,l} = M_{\gamma,l}/\delta$. Furthermore for constant $\tau_l > 0$, $\Psi_l : \mathbb{R} \times \Omega_l \to \mathbb{R}$ is Lipschitz continuous, strictly monotonically decreasing in the first variable, and it holds $|\Psi_l(p, x) - \Psi_l(q, x)| \leq L_{\Psi,l} |p - q|$ for all $p, q \in \mathbb{R}$, where $L_{\Psi,l} = \tau_l^{-1}$.

The system of nonlinear equations (2.1)–(2.4) with either (2.6) or (2.7) forms an initial-boundary-value problem in the primary variables s, p_n and p_w for given initial data $s|_{t=0} = s^0 \in L^\infty(\Omega; [0, 1])$.

Remark 2.5 (Existence and boundedness of unique weak solutions). For the existence of unique weak solutions to (2.1)–(2.4) under either condition (2.6) or (2.7), with respect to initial and boundary conditions, we refer to [48, 49, 57]. The existence of solutions was proved in [48], while the uniqueness of the solutions to these equations

for $\delta = 0$ was derived in [49, 57]. Note that additional assumptions on the regularity of the coefficient functions and the domain are necessary for this. Furthermore, the sequence of solutions to the regularized equations converge (weakly) towards the solution of the original equations for $\delta \to 0$, as shown in [50]. For the following analysis, we emphasize that $s \in L^\infty(0,T;C^{0,\alpha}(\overline{\Omega}))$ and $p_n, p_w \in L^\infty(0,T;C^{1,\alpha}(\overline{\Omega}))$ was proved in [49, Thm. 2.1] under the above-mentioned regularity assumptions.

3. Temporal Discretization and Iterative Schemes

First, we present the discretization in time by the θ-scheme. In particular, we are interested in the unconditionally stable situation when $\theta \geq 1/2$. For $\theta = 1$, this boils down to the first-order backward Euler method, while $\theta = 1/2$ coincides with the second-order Crank-Nicolson method. The resulting semi-discrete equations are nonlinear, and thus iterative methods are necessary to find the solutions. Therefore, we propose two linearization and domain decomposition schemes (LDD-schemes).

3.1. Discretization in Time

For given $N \in \mathbb{N}$, let the fixed time step length be $\Delta t := \frac{T}{N}$. At time $t^k := k\Delta t$, the approximations of the saturation, pressures and source terms are denoted $s^k, p_\alpha^k, q_\alpha^k$. With this, the auxiliary quantities at time t^k are

$$\mathbf{u}_{\alpha,l}^k := -\lambda_{\alpha,l}(s_l^k)K_l\nabla p_{\alpha,l}^k, \qquad p_{c,l}^k := p_{c,l}(s_l^k), \qquad \Psi_l^k := \Psi_l(p_{n,l}^k - p_{w,l}^k - p_{c,l}^k).$$

For $\theta \in (0,1]$, the θ-averaged quantities are defined by $(\cdot)^{k,\theta} := \theta(\cdot)^k + (1-\theta)(\cdot)^{k-1}$, e.g. $\mathbf{u}_{\alpha,l}^{k,\theta} = \theta\mathbf{u}_{\alpha,l}^k + (1-\theta)\mathbf{u}_{\alpha,l}^{k-1}$. Then, the interface conditions (2.4) directly become

$$\mathbf{u}_{\alpha,1}^{k,\theta}\cdot\nu_1 = -\mathbf{u}_{\alpha,2}^{k,\theta}\cdot\nu_2, \qquad p_{\alpha,1}^k = p_{\alpha,2}^k \qquad \text{on } \Gamma. \tag{3.1}$$

The time-discrete counterparts of (2.1) and (2.2) are tested with $\psi_n, \psi_w \in H_0^1(\Omega)$. After partial integration using (3.1) and summation over $l \in \{1,2\}$, the time-discrete, weak equations read

$$\sum_{l=1}^{2}\Big(-\phi_l\Big(\tfrac{s_l^k - s_l^{k-1}}{\Delta t},\ \psi_{n,l}\Big)_{\Omega_l} - \big(\mathbf{u}_{n,l}^{k,\theta},\ \nabla\psi_{n,l}\big)_{\Omega_l}\Big) = \big(q_{n,l}^{k,\theta},\ \psi_n\big)_\Omega, \tag{3.2}$$

$$\sum_{l=1}^{2}\Big(\phi_l\Big(\tfrac{s_l^k - s_l^{k-1}}{\Delta t},\ \psi_{w,l}\Big)_{\Omega_l} - \big(\mathbf{u}_{w,l}^{k,\theta},\ \nabla\psi_{w,l}\big)_{\Omega_l}\Big) = \big(q_{w,l}^{k,\theta},\ \psi_w\big)_\Omega, \tag{3.3}$$

$$p_{n,l}^{k,\theta} - p_{w,l}^{k,\theta} = p_{c,l}^{k,\theta} - \Phi_{\delta,l}\Big(\tfrac{s_l^k - s_l^{k-1}}{\Delta t}\Big) - \tfrac{T_l(s_l^k) - T_l(s_l^{k-1})}{\Delta t} \quad \text{in } L^2(\Omega_l) \text{ for } l \in \{1,2\}, \tag{3.4}$$

$$\tfrac{s_l^k - s_l^{k-1}}{\Delta t} = \theta\Psi_l^k + (1-\theta)\Psi_l^{k-1} \quad \text{in } L^2(\Omega_l) \text{ for } l \in \{1,2\}. \tag{3.5}$$

Observe that either (3.4) or (3.5) will be used below, and thus there are the following two semi-discrete formulations.

Problem 1 (Semi-discrete weak formulation I). Given $(s^{k-1}, p_n^{k-1}, p_w^{k-1}) \in \mathcal{V}$, find $(s^k, p_n^k, p_w^k) \in \mathcal{V}$ such that (3.2)–(3.4) hold for all $\psi_n, \psi_w \in H_0^1(\Omega)$.

Problem 2 (Semi-discrete weak formulation II). Given $(s^{k-1}, p_n^{k-1}, p_w^{k-1}) \in \mathcal{V}$, find $(s^k, p_n^k, p_w^k) \in \mathcal{V}$ such that (3.2), (3.3), and (3.5) hold for all $\psi_n, \psi_w \in H_0^1(\Omega)$.

In particular, the second formulation is well suited for hysteretic models. In the absence of hysteresis, the first formulation is more natural and can be straightforwardly used even for vanishing τ. Note that both weak semi-discrete problems are well defined.

Remark 3.1. If $(s^k, p_n^k, p_w^k) \in \mathcal{V}$ is a solution of Problem 1 or Problem 2, $p_{\alpha,1}^k|_\Gamma = p_{\alpha,2}^k|_\Gamma$ holds by the definition of $\mathcal{V}$. Since $s_l^k, s_l^{k-1}, q_\alpha^{k,\theta} \in L^2(\Omega_l)$, testing (3.2) and (3.3) with arbitrary $\psi_{\alpha,l} \in C_0^\infty(\Omega_l)$ implies $\nabla\cdot \mathbf{u}_{\alpha,l}^{k,\theta} \in L^2(\Omega_l)$, i.e. $\mathbf{u}_{\alpha,l}^{k,\theta} \in H^{\mathrm{div}}(\Omega_l)$. This shows that

$$\nabla\cdot \mathbf{u}_{n,l}^{k,\theta} = \phi_l \tfrac{s_l^k - s_l^{k-1}}{\Delta t} + q_{n,l}^{k,\theta}, \qquad \nabla\cdot \mathbf{u}_{w,l}^{k,\theta} = -\phi_l \tfrac{s_l^k - s_l^{k-1}}{\Delta t} + q_{w,l}^{k,\theta} \qquad \text{in } L^2(\Omega_l). \tag{3.6}$$

Therefore, the normal trace lemma [58, Lemma III.1.1] yields $\mathbf{u}_{\alpha,l}^{k,\theta}\cdot\nu_l \in H^{1/2}(\partial\Omega_l)'$ and integration by parts in (3.2) and (3.3) implies $\mathbf{u}_{\alpha,1}^{k,\theta}\cdot\nu_1 = -\mathbf{u}_{\alpha,2}^{k,\theta}\cdot\nu_2$ in $H_{00}^{1/2}(\Gamma)'$.

Problems 1 and 2 are nonlinear systems of mixed elliptic algebraic equations with possibly discontinuous coefficients. This is evident when (3.5) is substituted into (3.2) and (3.3). One may prove the existence of (unique) solutions analogously to the time-continuous case (Remark 2.5) or the fully discrete case in [59] for equilibrium capillary pressure. By this, the time-discrete pressure gradients should be bounded – corresponding to the results in [49, 59]. However, this lies out of the scope of this article.

3.2. Linearization and Domain Decomposition Schemes

To decouple the problems on the subdomains, and thereby to account for the possible discontinuities at the interface Γ, we introduce a non-overlapping domain decomposition method. Following the ideas in [11, 60], we combine the interface conditions (3.1) by a (free to be chosen) parameter $\mathcal{L}_\Gamma \in (0,\infty)$ to define

$$g_{\alpha,l} := \mathbf{u}_{\alpha,l}^{k,\theta}\cdot\nu_l - \mathcal{L}_\Gamma p_{\alpha,l}^k.$$

With these Robin type expressions, the interface conditions (3.1) at Γ read

$$g_{\alpha,3-l} = -2\mathcal{L}_\Gamma p_{\alpha,l}^k - g_{\alpha,l}$$

for $l \in \{1,2\}$. This formulation is equivalent to (3.1) for any $\mathcal{L}_\Gamma \neq 0$, cf. [22, Remark 1 & 2]. Assuming that for some $i \in \mathbb{N}$ the approximations $(s^{k,i-1}, p_n^{k,i-1}, p_w^{k,i-1}) \in \mathcal{W}$ and $g_{\alpha,l}^{i-1} \in L^2(\Gamma)^4$ for $l \in \{1,2\}$ and $\alpha \in \{n,w\}$ are known, the linearized fluxes and interface conditions are defined by

$$\mathbf{u}_{\alpha,l}^{k,\theta,i} := -\theta\lambda_{\alpha,l}(s_l^{k,i-1})K_l\nabla p_{\alpha,l}^{k,i} - (1-\theta)\mathbf{u}_{\alpha,l}^{k-1}, \qquad g_{\alpha,l}^i := -2\mathcal{L}_\Gamma p_{\alpha,3-l}^{k,i-1} - g_{\alpha,3-l}^{i-1}.$$

With these, (3.2) and (3.3) become linear and decouple into

$$-\phi_l\left(\tfrac{s_l^{k,i}-s_l^{k-1}}{\Delta t},\ \psi_{n,l}\right)_{\Omega_l} - \left(\mathbf{u}_{n,l}^{k,\theta,i},\ \nabla\psi_{n,l}\right)_{\Omega_l} + \left(\mathcal{L}_\Gamma p_{n,l}^{k,i} + g_{n,l}^i,\ \psi_{n,l}\right)_\Gamma = \left(q_{n,l}^{k,\theta},\ \psi_{n,l}\right)_{\Omega_l}, \tag{3.7}$$

$$\phi_l\left(\tfrac{s_l^{k,i}-s_l^{k-1}}{\Delta t},\ \psi_{w,l}\right)_{\Omega_l} - \left(\mathbf{u}_{w,l}^{k,\theta,i},\ \nabla\psi_{w,l}\right)_{\Omega_l} + \left(\mathcal{L}_\Gamma p_{w,l}^{k,i} + g_{w,l}^i,\ \psi_{w,l}\right)_\Gamma = \left(q_{w,l}^{k,\theta},\ \psi_{w,l}\right)_{\Omega_l}, \tag{3.8}$$

$$g_{\alpha,l}^i = -2\mathcal{L}_\Gamma p_{\alpha,3-l}^{k,i-1} - g_{\alpha,3-l}^{i-1} \quad \text{in } L^2(\Gamma). \tag{3.9}$$

For (3.7)–(3.9), we expect to iteratively find the solution of the semi-discrete equations, if the limit exists. Formally, one can show the following limit equivalence.

Lemma 3.1 (Limit equations). *Let $k \in \mathbb{N}$ be fixed and assume that $(s^k, p_n^k, p_w^k) \in \mathcal{W}$ and $g_{\alpha,l} \in H_{00}^{1/2}(\Gamma)'$ for $l \in \{1,2\}$ and $\alpha \in \{n,w\}$ exist, such that it holds*

$$-\phi_l \left(\tfrac{s_l^k - s_l^{k-1}}{\Delta t},\ \psi_{n,l} \right)_{\Omega_l} - \left(\mathbf{u}_{n,l}^{k,\theta},\ \nabla \psi_{n,l} \right)_{\Omega_l} + \left\langle \mathcal{L}_\Gamma p_{n,l}^k + g_{n,l},\ \psi_{n,l} \right\rangle_\Gamma = \left(q_{n,l}^{k,\theta},\ \psi_{n,l} \right)_{\Omega_l}, \tag{3.10}$$

$$\phi_l \left(\tfrac{s_l^k - s_l^{k-1}}{\Delta t},\ \psi_{w,l} \right)_{\Omega_l} - \left(\mathbf{u}_{w,l}^{k,\theta},\ \nabla \psi_{w,l} \right)_{\Omega_l} + \left\langle \mathcal{L}_\Gamma p_{w,l}^k + g_{w,l},\ \psi_{w,l} \right\rangle_\Gamma = \left(q_{w,l}^{k,\theta},\ \psi_{w,l} \right)_{\Omega_l}, \tag{3.11}$$

$$\langle g_{\alpha,l},\ \psi_{\alpha,l} \rangle_\Gamma = \left\langle -2\mathcal{L}_\Gamma p_{\alpha,3-l}^k - g_{\alpha,3-l},\ \psi_{\alpha,l} \right\rangle_\Gamma, \tag{3.12}$$

for $l \in \{1,2\}$ and all $\psi_n, \psi_w \in H_0^1(\Omega)$, as well as either (3.4) or (3.5). Then, the interface conditions $\mathbf{u}_{\alpha,1}^{k,\theta} \cdot \nu_1 = -\mathbf{u}_{\alpha,2}^{k,\theta} \cdot \nu_2$ in $H_{00}^{1/2}(\Gamma)'$ and $p_{\alpha,1}^k|_\Gamma = p_{\alpha,2}^k|_\Gamma$ are satisfied, and thus $(s^k, p_n^k, p_w^k) \in \mathcal{V}$ is a solution of Problem 1 or Problem 2, respectively. Moreover, it holds $g_{\alpha,l} = \mathbf{u}_{\alpha,l}^{k,\theta} \cdot \nu_l - \mathcal{L}_\Gamma p_{\alpha,l}^k$ in $H_{00}^{1/2}(\Gamma)'$.
Vice versa, if $(s^k, p_n^k, p_w^k) \in \mathcal{V}$ is a solution of Problem 1 or Problem 2, and we define

$$g_{\alpha,l} := \mathbf{u}_{\alpha,l}^{k,\theta} \cdot \nu_l - \mathcal{L}_\Gamma p_{\alpha,l}^k \qquad \text{in } H_{00}^{1/2}(\Gamma)', \tag{3.13}$$

then (s^k, p_n^k, p_w^k) and $g_{\alpha,l}$, $l \in \{1,2\}$ and $\alpha \in \{n,w\}$, solve the limit system (3.10)–(3.12).

Proof. Subtracting the equations (3.12) for $l \in \{1,2\}$ directly yields $p_{\alpha,1}^k|_\Gamma = p_{\alpha,2}^k|_\Gamma$, whereas adding up these equations leads to $g_{\alpha,1} + g_{\alpha,2} = -\mathcal{L}_\Gamma(p_{\alpha,1}^k + p_{\alpha,2}^k)$. Using this in the sum of (3.10) over $l \in \{1,2\}$ gives (3.2). Analogously, one obtains (3.3) from (3.11). Together with (3.4) or (3.5), this is equivalent to Problem 1 or Problem 2, respectively. Furthermore, integration by parts in (3.10) and (3.11) using (3.6) leads to $g_{\alpha,l} = \mathbf{u}_{\alpha,l}^{k,\theta} \cdot \nu_l - \mathcal{L}_\Gamma p_{\alpha,l}^k$ in $H_{00}^{1/2}(\Gamma)'$.
Conversely, if (s^k, p_n^k, p_w^k) solves Problem 1 or Problem 2, then the continuity of pressures and normal fluxes at Γ holds, and thus one gets

$$g_{\alpha,l} = \mathbf{u}_{\alpha,l}^{k,\theta} \cdot \nu_l - \mathcal{L}_\Gamma p_{\alpha,l}^k = -\mathbf{u}_{\alpha,3-l}^{k,\theta} \cdot \nu_{3-l} - \mathcal{L}_\Gamma p_{\alpha,3-l}^k = -2\mathcal{L}_\Gamma p_{\alpha,3-l}^k - g_{\alpha,3-l}$$

in $H_{00}^{1/2}(\Gamma)'$. Finally, (3.10) and (3.11) follow from partial integration of (3.2) and (3.3) using (3.6) and the definition of $g_{\alpha,l}$. □

The above-shown equivalence of Lemma 3.1 can also be observed for Richards' equation [22]. We will use this formal limit (3.10)–(3.12) to prove that the solutions to the LDD-schemes converge towards the solutions of the semi-discrete Problems 1 and 2. Although this convergence is independent of the initial guess, as shown below in Theorems 4.1 and 4.2, note that the natural choices for the first iteration are

$$s_l^{k,0} := s_l^{k-1}, \qquad p_{\alpha,l}^{k,0} := p_{\alpha,l}^{k-1}, \qquad g_{\alpha,l}^0 := \mathbf{u}_{\alpha,l}^{k-1} \cdot \nu_l - \mathcal{L}_\Gamma p_{\alpha,l}^{k-1}.$$

The two problems only differ in the used capillary pressure relation, but this will result in different iterative schemes, as will be seen below. Since the used strategies

differ, we present each LDD-scheme individually. Nevertheless, the common idea is to linearize the capillary pressure equations (3.4) and (3.5), and to add stabilization terms of the form

$$\mathcal{L}(\text{solution of current iteration} - \text{solution of last iteration}),$$

which vanish in the limit if the sequence converges.

For Problem 1, we use the stabilization parameters $\mathcal{L}_{p,l}, \mathcal{L}_{\Phi,l}, \mathcal{L}_{T,l} \geq 0$, which must satisfy some mild constraints to guarantee convergence, as shown below in Theorem 4.1. With these, the stabilized linearization of (3.4) becomes

$$\begin{aligned} p_{n,l}^{k,\theta,i} - p_{w,l}^{k,\theta,i} + \left(\mathcal{L}_{p,l} + \tfrac{\mathcal{L}_{T,l}+\mathcal{L}_{\Phi,l}}{\Delta t}\right)(s_l^{k,i} - s_l^{k,i-1}) = \theta p_{c,l}(s_l^{k,i-1}) + (1-\theta)p_{c,l}^{k-1} \\ -\Phi_{\delta,l}\left(\tfrac{s_l^{k,i-1}-s_l^{k-1}}{\Delta t}\right) - \tfrac{T_l(s_l^{k,i-1})-T_l(s_l^{k-1})}{\Delta t} \quad \text{in } L^2(\Omega_l), \end{aligned} \tag{3.14}$$

for $l \in \{1,2\}$, where $p_{\alpha,l}^{k,\theta,i} := \theta p_{\alpha,l}^{k,i} + (1-\theta)p_{\alpha,l}^{k-1}$. Clearly, the stabilizing term in (3.14) vanishes in the case of convergence, and hence the formal limit is (3.4). The iteration reduces to solving the following problem.

Problem 3 (Weak formulation of the LDD-scheme I). Given $(s^{k-1}, p_n^{k-1}, p_w^{k-1}) \in \mathcal{V}$, $(s^{k,i-1}, p_n^{k,i-1}, p_w^{k,i-1}) \in \mathcal{W}$ and $g_{\alpha,l}^{i-1} \in L^2(\Gamma)$ for $l \in \{1,2\}$, $\alpha \in \{n,w\}$, find $(s^{k,i}, p_n^{k,i}, p_w^{k,i}) \in \mathcal{W}$ and $g_{\alpha,l}^{i} \in L^2(\Gamma)$ for $l \in \{1,2\}$ and $\alpha \in \{n,w\}$, such that the equations (3.7)–(3.9) and (3.14) hold for all $\psi_{n,l}, \psi_{w,l} \in \mathcal{W}_l$ and $l \in \{1,2\}$.

For Problem 2, we define the semi-linearized inverted capillary pressure equation based on (3.5) and $\Psi_l^{k,i} := \Psi_l(p_{n,l}^{k,i-1} - p_{w,l}^{k,i-1} - p_{c,l}(s_l^{k,i}))$ by

$$\tfrac{s_l^{k,i}-s_l^{k-1}}{\Delta t} = \theta\Psi_l^{k,i} + (1-\theta)\Psi_l^{k-1} \quad \text{in } L^2(\Omega_l) \text{ for } l \in \{1,2\}. \tag{3.15}$$

Note that $s_l^{k,i}$ still arises implicitly. However, (3.15) defines a contraction, as shown in Lemma 4.2. Therefore, it can be easily solved by directly applying the associated fixed-point iteration or any other suited method such as the Newton-Raphson iteration.

Note that this allows to use $s_l^{k,i}$ for the definition of the flux

$$\mathbf{u}_{\alpha,l}^{k,\theta,i} - \theta\lambda_{\alpha,l}(s_l^{k,i})K_l\nabla p_{\alpha,l}^{k,i} - (1-\theta)\mathbf{u}_{\alpha,l}^{k-1}.$$

Substitution of (3.15) into (3.7) and (3.8) leads then to a nonlinear elliptic system of equation in $p_{n,l}$ and $p_{w,l}$. Therefore, we stabilize these equations using only one stabilization parameter $\mathcal{L}_{p,l} > 0$, which again must satisfy a mild constraint discussed in Section 4.2. In particular, the term $\mathcal{L}_{p,l}(p_{n,l}^{k,i} - p_{n,l}^{k,i-1} - p_{w,l}^{k,i} + p_{w,l}^{k,i-1})$ is added to (3.7) and subtracted from (3.8). Again, this term vanishes in case of convergence. Altogether, the second LDD-scheme is constituted by iteratively solving the following problem.

Problem 4 (Weak formulation of the LDD-scheme II). Given $(s^{k-1}, p_n^{k-1}, p_w^{k-1}) \in \mathcal{V}$, $(s^{k,i-1}, p_n^{k,i-1}, p_w^{k,i-1}) \in \mathcal{W}$ and $g_{\alpha,l}^{i-1} \in L^2(\Gamma)$ for $l \in \{1,2\}$, $\alpha \in \{n,w\}$, find $(s^{k,i}, p_n^{k,i}, p_w^{k,i}) \in$

$\mathcal{W}$ and $g^i_{\alpha,l} \in L^2(\Gamma)$ for $l \in \{1,2\}$, $\alpha \in \{n,w\}$, such that it holds

$$-\phi_l\left(\tfrac{s_l^{k,i}-s_l^{k-1}}{\Delta t},\ \psi_{n,l}\right)_{\Omega_l} + \mathcal{L}_{p,l}\left(p_{n,l}^{k,i} - p_{n,l}^{k,i-1} - p_{w,l}^{k,i} + p_{w,l}^{k,i-1},\ \psi_{n,l}\right)_{\Omega_l}$$
$$-\left(\mathbf{u}_{n,l}^{k,\theta,i},\ \nabla\psi_{n,l}\right)_{\Omega_l} + \left(\mathcal{L}_\Gamma p_{n,l}^{k,i} + g_{n,l}^i,\ \psi_{n,l}\right)_\Gamma = \left(q_{n,l}^{k,\theta},\ \psi_{n,l}\right)_{\Omega_l}, \tag{3.16}$$

$$\phi_l\left(\tfrac{s_l^{k,i}-s_l^{k-1}}{\Delta t},\ \psi_{w,l}\right)_{\Omega_l} - \mathcal{L}_{p,l}\left(p_{n,l}^{k,i} - p_{n,l}^{k,i-1} - p_{w,l}^{k,i} + p_{w,l}^{k,i-1},\ \psi_{w,l}\right)_{\Omega_l}$$
$$-\left(\mathbf{u}_{w,l}^{k,\theta,i},\ \nabla\psi_{w,l}\right)_{\Omega_l} + \left(\mathcal{L}_\Gamma p_{w,l}^{k,i} + g_{w,l}^i,\ \psi_{w,l}\right)_\Gamma = \left(q_{w,l}^{k,\theta},\ \psi_{w,l}\right)_{\Omega_l}, \tag{3.17}$$

$$g^i_{\alpha,l} = -2\mathcal{L}_\Gamma p^{k,i-1}_{\alpha,3-l} - g^{i-1}_{\alpha,3-l} \quad \text{in } L^2(\Gamma), \tag{3.18}$$

$$\tfrac{s_l^{k,i}-s_l^{k-1}}{\Delta t} = \theta\Psi_l^{k,i} + (1-\theta)\Psi_l^{k-1} \quad \text{in } L^2(\Omega_l), \tag{3.19}$$

for all $\psi_{n,l}, \psi_{w,l} \in \mathcal{W}_l$ and $l \in \{1,2\}$.

4. Existence and Convergence of the Solutions to the LDD-schemes

In the following, Problems 3 and 4 defining the LDD-schemes are analyzed. The existence of unique solutions to these problems and the convergence towards the solutions of the semi-discrete equations is rigorously proved. The ideas of the proofs are based on [5, 22, 23], where similar models are discussed, in which either hysteresis or both dynamic capillarity and hysteresis are absent. In comparison to [24], the proofs are generalized and corrected. The LDD-scheme I is presented first, the second one afterwards.

4.1. Existence and Convergence of the Solutions to the LDD-scheme I

The existence of a unique solution to Problem 3 is a direct consequence of the linearization.

Lemma 4.1. *Problem 3 has a unique solution if Assumption 1 is fulfilled and* $\theta \in (0,1]$.

Proof. Since $p^{k,i-1}_{\alpha,l}|_\Gamma \in L^2(\Gamma)$, (3.9) yields unique $g^i_{\alpha,l} \in L^2(\Gamma)$ for $l \in \{1,2\}$ and $\alpha \in \{n,w\}$. Further, (3.14) can be rewritten as

$$\tfrac{s_l^{k,i}-s_l^{k-1}}{\Delta t} = -\beta_l(p_{n,l}^{k,i} - p_{w,l}^{k,i}) + f_l^i \quad \text{in } L^2(\Omega_l), \tag{4.1}$$

where $\beta_l = \theta(\mathcal{L}_{p,l}\Delta t + \mathcal{L}_{T,l} + \mathcal{L}_{\Phi,l})^{-1} > 0$, and f_l^i is independent of any quantity at the iteration i. Inserting this into the sum of (3.7) and (3.8) leads to

$$\phi_l\beta_l\left(p_{n,l}^{k,i} - p_{w,l}^{k,i},\ \psi_{n,l} - \psi_{w,l}\right)_{\Omega_l} + \theta\sum_{\alpha\in\{n,w\}}\left(\lambda_{\alpha,l}(s_l^{k,i-1})K_l\nabla p_{\alpha,l}^{k,i},\ \nabla\psi_{\alpha,l}\right)_{\Omega_l}$$
$$+\sum_{\alpha\in\{n,w\}}\mathcal{L}_\Gamma\left(p_{\alpha,l}^{k,i},\ \psi_{\alpha,l}\right)_\Gamma = \sum_{\alpha\in\{n,w\}}\left(f_{\alpha,l}^i,\ \psi_{\alpha,l}\right)_{\Omega_l} - \sum_{\alpha\in\{n,w\}}\left(g_{\alpha,l}^i,\ \psi_{\alpha,l}\right)_\Gamma,$$

where $f^i_{\alpha,l} \in L^2(\Omega_l)$ is independent of any quantity at iteration i for both $\alpha \in \{n,w\}$. By the Lax-Milgram lemma, a unique solution $(p^{k,i}_{n,l}, p^{k,i}_{w,l}) \in [\mathcal{W}_l]^2$ exists for $l \in \{1,2\}$. Finally, $s_l^{k,i} \in L^2(\Omega_l)$ is uniquely determined by (4.1). □

To prove the convergence of the LDD-scheme I, we derive a-priory estimates for the errors between the solution to Problem 3 and the solution of the limit equations. These estimates yield the convergence for any initial guess.

Theorem 4.1 (Convergence of the LDD-scheme I). *Let Assumption 1 be fulfilled and $\theta \in (0,1]$. Assume that a solution $(s^k, p_n^k, p_w^k) \in \mathcal{V}$ of Problem 1 exists and satisfies $\left\|K_l^{1/2}\nabla p_{\alpha,l}^k\right\|_{L^\infty(\Omega_l)} \leq M_{p_\alpha,l}$ and $\mathbf{u}_{\alpha,l}^{k,\theta}\cdot\nu_l \in L^2(\Gamma)$. If the stabilization parameters are sufficiently large and the time step is small enough, i.e.*

$$\mathcal{L}_{p,l} \geq \tfrac{L_{p_c,l}}{\theta}, \qquad \mathcal{L}_{T,l} \geq \tfrac{L_{T,l}}{2}, \qquad \mathcal{L}_{\Phi,l} \geq \tfrac{L_{\Phi_\delta,l}}{2} \qquad \text{and} \qquad \Delta t < \frac{\phi_l m_{p_c,l}}{\sum\limits_{\alpha\in\{n,w\}} \frac{\theta L_{\lambda_\alpha,l}^2 M_{p_\alpha,l}^2}{m_{\lambda_\alpha,l}}},$$

for $l \in \{1,2\}$, the sequence of solutions of Problem 3 converges towards the solution of Problem 1 independently of the initial guess $(s^{k,0}, p_n^{k,0}, p_w^{k,0}) \in \mathcal{W}$ and $g_{\alpha,l}^0 \in L^2(\Gamma)$ for $l \in \{1,2\}$ and $\alpha \in \{n,w\}$. More precisely, it holds

$$s_l^{k,i} \to s_l^k \ \text{ in } \ L^2(\Omega_l), \qquad p_{\alpha,l}^{k,i} \to p_{\alpha,l}^k \ \text{ in } \ \mathcal{W}_l, \qquad g_{\alpha,l}^i \rightharpoonup g_{\alpha,l} \ \text{ in } \ L^2(\Gamma)$$

for $l \in \{1,2\}$ and $\alpha \in \{n,w\}$ as $i \to \infty$.

Remark 4.1. Due to the regularized sign-function, one has $L_{\Phi_\delta,l} = M_{\gamma,l}/\delta$. This means that the stabilization parameters and the time step can be chosen independently of the regularization, except for $\mathcal{L}_{\Phi,l} \geq M_{\gamma,l}/(2\delta)$.

Remark 4.2. The assumptions on the solution of Problem 1 seem rather restrictive, but as mentioned in Remark 2.5, the solution is expected to fulfill $s_l^k \in C^0(\overline{\Omega_l})$ and $p_{\alpha,l}^k \in C^1(\overline{\Omega_l})$. Then, one would have $\lambda_{\alpha,l}(s_l^k)\nabla p_{\alpha,l}^k \in C^0(\overline{\Omega_l})$ and hence these assumptions would be always fulfilled.

Proof (Theorem 4.1). The iteration errors are defined by

$$e_{s,l}^i := s_l^{k,i} - s_l^k \in L^2(\Omega_l), \quad e_{p_\alpha,l}^i := p_{\alpha,l}^{k,i} - p_{\alpha,l}^k \in \mathcal{W}_l, \quad e_{g_\alpha,l}^i := g_{\alpha,l}^i - g_{\alpha,l} \in L^2(\Gamma).$$

Subtraction of the limit equations (3.4) and (3.10)–(3.12) from (3.7)–(3.9) and (3.14) leads to

$$\begin{aligned}
-\phi_l\left(\tfrac{e_{s,l}^i}{\Delta t},\, \psi_{n,l}\right)_{\Omega_l} &+ \theta\left(\lambda_{n,l}(s_l^{k,i-1})K_l\nabla p_{n,l}^{k,i} - \lambda_{n,l}(s_l^k)K_l\nabla p_{n,l}^k,\, \nabla\psi_{n,l}\right)_{\Omega_l} \\
&+ \left(\mathcal{L}_\Gamma e_{p_n,l}^i + e_{g_n,l}^i,\, \psi_{n,l}\right)_\Gamma = 0, \qquad (4.2)\\
\phi_l\left(\tfrac{e_{s,l}^i}{\Delta t},\, \psi_{w,l}\right)_{\Omega_l} &+ \theta\left(\lambda_{w,l}(s_l^{k,i-1})K_l\nabla p_{w,l}^{k,i} - \lambda_{w,l}(s_l^k)K_l\nabla p_{w,l}^k,\, \nabla\psi_{w,l}\right)_{\Omega_l} \\
&+ \left(\mathcal{L}_\Gamma e_{p_w,l}^i + e_{g_w,l}^i,\, \psi_{w,l}\right)_\Gamma = 0, \qquad (4.3)\\
e_{g_\alpha,l}^i &= -2\mathcal{L}_\Gamma e_{p_\alpha,3-l}^{i-1} - e_{g_\alpha,3-l}^{i-1} \quad \text{in } L^2(\Gamma), \qquad (4.4)\\
\theta(e_{p_n,l}^i - e_{p_w,l}^i) + \left(\mathcal{L}_{p,l} + \tfrac{\mathcal{L}_{T,l}+\mathcal{L}_{\Phi,l}}{\Delta t}\right)(e_{s,l}^i - e_{s,l}^{i-1}) &= \theta(p_{c,l}(s_l^{k,i-1}) - p_{c,l}(s_l^k)) \\
-\tfrac{T_l(s_l^{k,i-1}) - T_l(s_l^k)}{\Delta t} - \left(\Phi_{\delta,l}\left(\tfrac{s_l^{k,i-1}-s_l^{k-1}}{\Delta t}\right) - \Phi_{\delta,l}\left(\tfrac{s_l^k - s_l^{k-1}}{\Delta t}\right)\right) &\quad \text{in } L^2(\Omega_l). \qquad (4.5)
\end{aligned}$$

Error estimate on the interface conditions. Using (4.4), the norm of $e^i_{g_\alpha,l}$ is

$$\left\|e^i_{g_\alpha,l}\right\|^2_\Gamma = 4\mathcal{L}_\Gamma\left(\mathcal{L}_\Gamma e^{i-1}_{p_\alpha,3-l} + e^{i-1}_{g_\alpha,3-l},\ e^{i-1}_{p_\alpha,3-l}\right)_\Gamma + \left\|e^{i-1}_{g_\alpha,3-l}\right\|^2_\Gamma$$

and thus by index shifting i to $i+1$ and l to $3-l$

$$\left(\mathcal{L}_\Gamma e^i_{p_\alpha,l} + e^i_{g_\alpha,l},\ e^{i-1}_{p_\alpha,3-l}\right)_\Gamma = -\frac{1}{4\mathcal{L}_\Gamma}\left(\left\|e^i_{g_\alpha,l}\right\|^2_\Gamma - \left\|e^{i+1}_{g_\alpha,3-l}\right\|^2_\Gamma\right). \tag{4.6}$$

Error estimate on the non-wetting pressure. Testing (4.2) with $\psi_{n,l} = e^i_{p_n,l}$ yields

$$\begin{aligned}-\phi_l\left(\tfrac{e^i_{s,l}}{\Delta t},\ e^i_{p_n,l}\right)_{\Omega_l} &+ \theta\left(\lambda_{n,l}(s^{k,i-1}_l)K_l\nabla e^i_{p_n,l},\ \nabla e^i_{p_n,l}\right)_{\Omega_l} + \left(\mathcal{L}_\Gamma e^i_{p_n,l} + e^i_{g_n,l},\ e^i_{p_n,l}\right)_\Gamma\\ &+ \theta\left((\lambda_{n,l}(s^{k,i-1}_l) - \lambda_{n,l}(s^k_l))K_l\nabla p^k_{n,l},\ \nabla e^i_{p_n,l}\right)_{\Omega_l} = 0.\end{aligned}$$

Since $\lambda_{n,l}$ has the lower bound $m_{\lambda_n,l}$ and is Lipschitz continuous, one obtains with the Cauchy-Schwarz inequality and (4.6)

$$\begin{aligned}-\phi_l\left(\tfrac{e^i_{s,l}}{\Delta t},\ e^i_{p_n,l}\right)_{\Omega_l} &+ \theta m_{\lambda_n,l}\left\|K_l^{1/2}\nabla e^i_{p_n,l}\right\|^2_{\Omega_l} - \frac{1}{4\mathcal{L}_\Gamma}\left(\left\|e^i_{g_\alpha,l}\right\|^2_\Gamma - \left\|e^{i+1}_{g_\alpha,3-l}\right\|^2_\Gamma\right)\\ &\le \theta L_{\lambda_n,l}\left\|K_l^{1/2}\nabla p^k_{n,l}\right\|_{L^\infty(\Omega_l)}\left\|e^{i-1}_{s,l}\right\|_{\Omega_l}\left\|K_l^{1/2}\nabla e^i_{p_n,l}\right\|_{\Omega_l}.\end{aligned}$$

By Young's inequality and the bound on the pressure gradient, one gets

$$\begin{aligned}-\phi_l\left(\tfrac{e^i_{s,l}}{\Delta t},\ e^i_{p_n,l}\right)_{\Omega_l} &+ \frac{\theta m_{\lambda_n,l}}{2}\left\|K_l^{1/2}\nabla e^i_{p_n,l}\right\|^2_{\Omega_l}\\ &\le \frac{\theta L^2_{\lambda_n,l}M^2_{p_n,l}}{2m_{\lambda_n,l}}\left\|e^{i-1}_{s,l}\right\|^2_{\Omega_l} + \frac{1}{4\mathcal{L}_\Gamma}\left(\left\|e^i_{g_\alpha,l}\right\|^2_\Gamma - \left\|e^{i+1}_{g_\alpha,3-l}\right\|^2_\Gamma\right).\end{aligned} \tag{4.7}$$

Error estimate on the wetting pressure. Testing (4.3) with $\psi_{w,l} = e^i_{p_w,l}$ and following the same steps as for the non-wetting pressure equation yields

$$\begin{aligned}\phi_l\left(\tfrac{e^i_{s,l}}{\Delta t},\ e^i_{p_w,l}\right)_{\Omega_l} &+ \frac{\theta m_{\lambda_w,l}}{2}\left\|K_l^{1/2}\nabla e^i_{p_w,l}\right\|^2_{\Omega_l}\\ &\le \frac{\theta L^2_{\lambda_w,l}M^2_{p_w,l}}{2m_{\lambda_w,l}}\left\|e^{i-1}_{s,l}\right\|^2_{\Omega_l} + \frac{1}{4\mathcal{L}_\Gamma}\left(\left\|e^i_{g_w,l}\right\|^2_\Gamma - \left\|e^{i+1}_{g_w,3-l}\right\|^2_\Gamma\right).\end{aligned} \tag{4.8}$$

Error estimate on the pressure difference. Testing (4.5) with $\psi_{p,l} = e^i_{s,l}$ and using the identity $a(a-b) = \frac{1}{2}(a^2 - b^2 + (a-b)^2)$ for the stabilization term yields

$$\begin{aligned}&\theta\left(e^i_{p_n,l} - e^i_{p_w,l},\ e^i_{s,l}\right)_{\Omega_l} + \left(\tfrac{\mathcal{L}_{p,l}}{2} + \tfrac{\mathcal{L}_{T,l}+\mathcal{L}_{\Phi,l}}{2\Delta t}\right)\left(\left\|e^i_{s,l}\right\|^2_{\Omega_l} - \left\|e^{i-1}_{s,l}\right\|^2_{\Omega_l} + \left\|e^i_{s,l} - e^{i-1}_{s,l}\right\|^2_{\Omega_l}\right)\\ &= \left(\theta\left(p_{c,l}(s^{k,i-1}_l) - p_{c,l}(s^k_l)\right) - \tfrac{T_l(s^{k,i-1}_l) - T_l(s^k_l)}{\Delta t},\ e^{i-1}_{s,l}\right)_{\Omega_l}\\ &\quad - \left(\Phi_{\delta,l}\left(\tfrac{s^{k,i-1}_l - s^{k-1}_l}{\Delta t}\right) - \Phi_{\delta,l}\left(\tfrac{s^k_l - s^{k-1}_l}{\Delta t}\right),\ e^{i-1}_{s,l}\right)_{\Omega_l}\\ &\quad + \left(\theta\left(p_{c,l}(s^{k,i-1}_l) - p_{c,l}(s^k_l)\right) - \tfrac{T_l(s^{k,i-1}_l) - T_l(s^k_l)}{\Delta t},\ e^i_{s,l} - e^{i-1}_{s,l}\right)_{\Omega_l}\\ &\quad - \left(\Phi_{\delta,l}\left(\tfrac{s^{k,i-1}_l - s^{k-1}_l}{\Delta t}\right) - \Phi_{\delta,l}\left(\tfrac{s^k_l - s^{k-1}_l}{\Delta t}\right),\ e^i_{s,l} - e^{i-1}_{s,l}\right)_{\Omega_l}.\end{aligned}$$

Since $p_{c,l}$, T_l and $\Phi_{\delta,l}$ are Lipschitz-continuous and monotone, one gets

$$\begin{aligned}
&\theta\left(e^i_{p_n,l}-e^i_{p_w,l},\ e^i_{s,l}\right)_{\Omega_l}+\left(\tfrac{\mathcal{L}_{p,l}}{2}+\tfrac{\mathcal{L}_{T,l}+\mathcal{L}_{\Phi,l}}{2\Delta t}\right)\left(\left\|e^i_{s,l}\right\|^2_{\Omega_l}-\left\|e^{i-1}_{s,l}\right\|^2_{\Omega_l}+\left\|e^i_{s,l}-e^{i-1}_{s,l}\right\|^2_{\Omega_l}\right)\\
&\quad+\tfrac{\theta}{2}\left(\left|p_{c,l}(s_l^{k,i-1})-p_{c,l}(s_l^k)\right|,\ \left|e^{i-1}_{s,l}\right|\right)_{\Omega_l}+\tfrac{\theta}{2L_{p_c,l}}\left\|p_{c,l}(s_l^{k,i-1})-p_{c,l}(s_l^k)\right\|^2_{\Omega_l}\\
&\quad+\tfrac{\Delta t}{L_{\Phi_\delta,l}}\left\|\Phi_{\delta,l}\left(\tfrac{s_l^{k,i-1}-s_l^{k-1}}{\Delta t}\right)-\Phi_{\delta,l}\left(\tfrac{s_l^k-s_l^{k-1}}{\Delta t}\right)\right\|^2_{\Omega_l}+\tfrac{\Delta t}{L_{T,l}}\left\|\tfrac{T_l(s_l^{k,i-1})-T_l(s_l^k)}{\Delta t}\right\|^2_{\Omega_l}\\
&\quad\le\left(\theta\left\|p_{c,l}(s_l^{k,i-1})-p_{c,l}(s_l^k)\right\|_{\Omega_l}+\left\|\tfrac{T_l(s_l^{k,i-1})-T_l(s_l^k)}{\Delta t}\right\|_{\Omega_l}\right.\\
&\qquad\left.+\left\|\Phi_{\delta,l}\left(\tfrac{s_l^{k,i-1}-s_l^{k-1}}{\Delta t}\right)-\Phi_{\delta,l}\left(\tfrac{s_l^k-s_l^{k-1}}{\Delta t}\right)\right\|_{\Omega_l}\right)\left\|e^i_{s,l}-e^{i-1}_{s,l}\right\|_{\Omega_l}.
\end{aligned}$$

Using the lower bound on the decrease of $p_{c,l}$ and Young's inequality, one obtains

$$\begin{aligned}
&\theta\left(e^i_{p_n,l}-e^i_{p_w,l},\ e^i_{s,l}\right)_{\Omega_l}+\left(\tfrac{\mathcal{L}_{p,l}}{2}+\tfrac{\mathcal{L}_{T,l}+\mathcal{L}_{\Phi,l}}{2\Delta t}\right)\left(\left\|e^i_{s,l}\right\|^2_{\Omega_l}-\left\|e^{i-1}_{s,l}\right\|^2_{\Omega_l}\right)+\tfrac{\theta m_{p_c,l}}{2}\left\|e^{i-1}_{s,l}\right\|^2_{\Omega_l}\\
&\quad\le\left(\tfrac{\theta^2}{2\mathcal{L}_{p,l}}-\tfrac{\theta}{2L_{p_c,l}}\right)\left\|p_{c,l}(s_l^{k,i-1})-p_{c,l}(s_l^k)\right\|^2_{\Omega_l}+\left(\tfrac{\Delta t}{2\mathcal{L}_{T,l}}-\tfrac{\Delta t}{L_{T,l}}\right)\left\|\tfrac{T_l(s_l^{k,i-1})-T_l(s_l^k)}{\Delta t}\right\|^2_{\Omega_l}\\
&\qquad+\left(\tfrac{\Delta t}{2\mathcal{L}_{\Phi,l}}-\tfrac{\Delta t}{L_{\Phi_\delta,l}}\right)\left\|\Phi_{\delta,l}\left(\tfrac{s_l^{k,i-1}-s_l^{k-1}}{\Delta t}\right)-\Phi_{\delta,l}\left(\tfrac{s_l^k-s_l^{k-1}}{\Delta t}\right)\right\|^2_{\Omega_l}.
\end{aligned}$$

Since $\mathcal{L}_{p,l}\ge L_{p_c,l}/\theta$, $\mathcal{L}_{T,l}\ge L_{T,l}/2$ and $\mathcal{L}_{\Phi,l}\ge L_{\Phi_\delta,l}/2$ by assumption, the terms on the righthand side can be neglected. Multiplication with $\phi_l(\theta\Delta t)^{-1}$ finally leads to

$$\begin{aligned}
&\phi_l\left(e^i_{p_n,l}-e^i_{p_w,l},\ \tfrac{e^i_{s,l}}{\Delta t}\right)_{\Omega_l}+\tfrac{\phi_l m_{p_c,l}}{2\Delta t}\left\|e^{i-1}_{s,l}\right\|^2_{\Omega_l}\\
&\qquad\le\tfrac{\phi_l}{\theta\Delta t}\left(\tfrac{\mathcal{L}_{p,l}}{2}+\tfrac{\mathcal{L}_{T,l}+\mathcal{L}_{\Phi,l}}{2\Delta t}\right)\left(\left\|e^{i-1}_{s,l}\right\|^2_{\Omega_l}-\left\|e^i_{s,l}\right\|^2_{\Omega_l}\right).
\end{aligned}\tag{4.9}$$

Combined error estimate. Summation of the estimates (4.7)–(4.9) yields

$$\begin{aligned}
&\sum_{\alpha\in\{n,w\}}\tfrac{\theta m_{\lambda_\alpha,l}}{2}\left\|K_l^{1/2}\nabla e^i_{p_\alpha,l}\right\|^2_{\Omega_l}+C_l(\Delta t)\left\|e^{i-1}_{s,l}\right\|^2_{\Omega_l}\\
&\qquad\le\tfrac{1}{4\mathcal{L}_\Gamma}\sum_{\alpha\in\{n,w\}}\left(\left\|e^i_{g_\alpha,l}\right\|^2_\Gamma-\left\|e^{i+1}_{g_\alpha,3-l}\right\|^2_\Gamma\right)\\
&\qquad\quad+\tfrac{\phi_l}{\theta\Delta t}\left(\tfrac{\mathcal{L}_{p,l}}{2}+\tfrac{\mathcal{L}_{T,l}+\mathcal{L}_{\Phi,l}}{2\Delta t}\right)\left(\left\|e^{i-1}_{s,l}\right\|^2_{\Omega_l}-\left\|e^i_{s,l}\right\|^2_{\Omega_l}\right),
\end{aligned}$$

where by assumption

$$C_l(\Delta t)=\tfrac{\phi_l m_{p_c,l}}{2\Delta t}-\sum_{\alpha\in\{n,w\}}\tfrac{\theta L^2_{\lambda_\alpha,l}M^2_{p_\alpha,l}}{2m_{\lambda_\alpha,l}}>0.$$

By summing the estimates for $l\in\{1,2\}$ and $i=1,2,\dots,r$, one gets

$$\begin{aligned}
&\sum_{i=1}^r\sum_{l=1}^2\sum_{\alpha\in\{n,w\}}\tfrac{\theta m_{\lambda_\alpha,l}}{2}\left\|K_l^{1/2}\nabla e^i_{p_\alpha,l}\right\|^2_{\Omega_l}+\sum_{i=1}^r\sum_{l=1}^2 C_l(\Delta t)\left\|e^{i-1}_{s,l}\right\|^2_{\Omega_l}\\
&\qquad\le\tfrac{1}{4\mathcal{L}_\Gamma}\sum_{l=1}^2\sum_{\alpha\in\{n,w\}}\left\|e^1_{g_\alpha,l}\right\|^2_\Gamma+\tfrac{\phi_l}{\theta\Delta t}\sum_{l=1}^2\left(\tfrac{\mathcal{L}_{p,l}}{2}+\tfrac{\mathcal{L}_{T,l}+\mathcal{L}_{\Phi,l}}{2\Delta t}\right)\left\|e^0_{s,l}\right\|^2_{\Omega_l}.
\end{aligned}$$

Since the righthand side is independent of r, we conclude that the series on the left are absolutely convergent. Therefore, $s_l^{k,i} \to s_l^k$ in $L^2(\Omega_l)$ and the Poincaré inequality implies $p_{\alpha,l}^{k,i} \to p_{\alpha,l}^k$ in $\mathcal{W}_l$. To show the convergence of the $g_{\alpha,l}^i$, we consider again (4.2) and (4.3), and take the limit $i \to \infty$. By continuity one obtains

$$\lim_{i\to\infty} \left(e_{g_\alpha,l}^i,\ \psi_{\alpha,l}\right)_\Gamma = 0$$

for any $\psi_{\alpha,l} \in \mathcal{W}_l$. Since the trace operator is surjective onto $H_{00}^{1/2}(\Gamma)$, which is dense in $L^2(\Gamma)$, we conclude $e_{g_\alpha,l}^i \rightharpoonup 0$ in $L^2(\Gamma)$ as $i \to \infty$. Additionally, one can directly obtain $e_{g_\alpha,l}^i + e_{g_\alpha,3-l}^{i-1} \to 0$ in $L^2(\Gamma)$ by (4.4). □

4.2. Existence and Convergence of the Solutions to the LDD-scheme II

The existence of a unique solution to Problem 4 is again a consequence of the linearization, but using additionally the contraction property in (3.19).

Lemma 4.2. *Problem 4 has a unique solution if Assumption 1 is fulfilled, $\theta \in (0, 1]$, and it holds $\Delta t\theta L_{\Psi,l} L_{p_c,l} < 1$.*

Proof. Since $p_{\alpha,l}^{k,i-1}|_\Gamma \in L^2(\Gamma)$, (3.9) uniquely provides $g_{\alpha,l}^i \in L^2(\Gamma)$ for $\alpha \in n, w$ and $l \in \{1, 2\}$. After multiplying (3.19) by Δt and adding s_l^{k-1}, the lefthand side is $s_l^{k,i}$, while the righthand side, considered as function

$$F_l(s_l^{k,i}) := s_l^{k-1} + \Delta t\theta\Psi_l\left(p_{n,l}^{k,i-1} - p_{w,l}^{k,i-1} - p_{c,l}(s_l^{k,i})\right) + \Delta t(1-\theta)\Psi_l^{k-1} \tag{4.10}$$

maps $L^2(\Omega_l)$ into itself. Moreover, for $s, r \in L^2(\Omega_l)$, it holds

$$\left\|F_l(s) - F_l(r)\right\|_{\Omega_l} \le \Delta t\theta L_{\Psi,l} L_{p_c,l} \left\|s - r\right\|_{\Omega_l}.$$

By assumption $\Delta t\theta L_{\Psi,l} L_{p_c,l} < 1$, so F_l is a contraction, and the Banach fixed-point theorem yields the existence of a unique solution $s_l^{k,i} \in L^2(\Omega_l)$ to (3.19). Reordering of the sum of (3.16) and (3.17) leads to

$$\begin{aligned}\mathcal{L}_{p,l}\left(p_{n,l}^{k,i} - p_{w,l}^{k,i},\ \psi_{n,l} - \psi_{w,l}\right)_{\Omega_l} + \theta \sum_{\alpha\in\{n,w\}} \left(\lambda_{\alpha,l}(s_l^{k,i}) K_l \nabla p_{\alpha,l}^{k,i},\ \nabla\psi_{\alpha,l}\right)_{\Omega_l} \\ + \sum_{\alpha\in\{n,w\}} \left(\mathcal{L}_\Gamma p_{\alpha,l}^{k,i},\ \psi_{\alpha,l}\right)_\Gamma = \sum_{\alpha\in\{n,w\}} \left(f_{\alpha,l}^i,\ \psi_{\alpha,l}\right)_{\Omega_l} - \sum_{\alpha\in\{n,w\}} \left(g_{\alpha,l}^i,\ \psi_{\alpha,l}\right)_\Gamma,\end{aligned}$$

where both $f_{\alpha,l}^i \in L^2(\Omega_l)$ are independent of $p_{n,l}^{k,i}$ and $p_{w,l}^{k,i}$. By the Lax-Milgram lemma, a unique solution $(p_{n,l}^{k,i}, p_{w,l}^{k,i}) \in [\mathcal{W}_l]^2$ exists for $l \in \{1, 2\}$. □

To prove the convergence of the LDD-scheme II, we derive a-priory estimates for the errors between the solution to Problem 4 and the solution of the limit equations. These estimates then yield the convergence for any initial guess.

Theorem 4.2 (Convergence of the LDD-scheme II). *Let Assumption 1 be fulfilled, and let $\theta \in (0,1]$ and $\tau_l > 0$ be fixed. Assume, that a solution $(s^k, p_n^k, p_w^k) \in \mathcal{V}$ of Problem 2 satisfying $\left\|K_l^{1/2}\nabla p_{\alpha,l}^k\right\|_{L^\infty(\Omega_l)} \leq M_{p_\alpha,l}$ and $\mathbf{u}_{\alpha,l}^{k,\theta}\cdot\nu_l \in L^2(\Gamma)$ exists. If the stabilization parameter is sufficiently large and the time step is small enough, i.e.*

$$\mathcal{L}_{p,l} > 2\phi_l\theta L_{\Psi,l}, \quad \Delta t \leq \frac{1}{2\theta L_{\Psi,l}L_{p_c,l}} \quad \text{and} \quad \Delta t \leq \sqrt{\frac{\frac{1}{2\theta\phi_l L_{\Psi,l}} - \frac{1}{\mathcal{L}_{p,l}}}{\sum\limits_{\alpha\in\{n,w\}}\left(\frac{2\theta L_{\Psi,l}^2 L_{p_c,l}^2 C_{\Omega_l}^2}{m_{\lambda_\alpha,l}\underline{K}_l} + \frac{\theta L_{\lambda_\alpha,l}^2 M_{p\alpha,l}^2}{\phi_l^2 m_{\lambda_\alpha,l}}\right)}}$$

for $l \in \{1,2\}$, the sequence of solutions of Problem 4 converges towards the solution of Problem 2 independently of the initial guess $(s^{k,0}, p_n^{k,0}, p_w^{k,0}) \in \mathcal{W}$ and $g_{\alpha,l}^0 \in L^2(\Gamma)$ for $l \in \{1,2\}$ and $\alpha \in \{n,w\}$. More precisely, it holds

$$s_l^{k,i} \to s_l^k \ \text{ in } \ L^2(\Omega_l), \qquad p_{\alpha,l}^{k,i} \to p_{\alpha,l}^k \ \text{ in } \ \mathcal{W}_l, \qquad g_{\alpha,l}^i \rightharpoonup g_{\alpha,l} \ \text{ in } \ L^2(\Gamma)$$

for $l \in \{1,2\}$, $\alpha \in \{n,w\}$ as $i \to \infty$.

Remark 4.3. The assumptions on the solution of Problem 2 seem rather restrictive, but as mentioned in Remark 2.5, the solution is expected to fulfill $s_l^k \in C^0(\overline{\Omega_l})$ and $p_{\alpha,l}^k \in C^1(\overline{\Omega_l})$. Then, one would have $\lambda_{\alpha,l}(s_l^k)\nabla p_{\alpha,l}^k \in C^0(\overline{\Omega_l})$ and hence these assumptions would be always fulfilled.

Proof (Theorem 4.2). We definer the iteration errors by

$$e_{s,l}^i := s_l^{k,i} - s_l^k \in L^2(\Omega_l), \quad e_{p_\alpha,l}^i := p_{\alpha,l}^{k,i} - p_{\alpha,l}^k \in \mathcal{W}_l, \quad e_{g_\alpha,l}^i := g_{\alpha,l}^i - g_{\alpha,l} \in L^2(\Gamma),$$
$$e_{p_c,l}^i := e_{p_n,l}^i - e_{p_w,l}^i \in \mathcal{W}_l, \quad e_{\Psi,l}^i := \Psi_l^{k,i} - \Psi_l(p_{n,l}^k - p_{w,l}^k - p_{c,l}(s_l^{k,i})) \in L^2(\Gamma).$$

Subtracting the limit equations (3.5) and (3.10)–(3.12) from (3.16)–(3.19) gives

$$-\phi_l\left(\tfrac{e_{s,l}^i}{\Delta t}, \psi_{n,l}\right)_{\Omega_l} + \mathcal{L}_{p,l}\left(e_{p_c,l}^i - e_{p_c,l}^{i-1}, \psi_{n,l}\right)_{\Omega_l} - \left(\mathbf{u}_{n,l}^{k,\theta,i} - \mathbf{u}_{n,l}^{k,\theta}, \nabla\psi_{n,l}\right)_{\Omega_l}$$
$$+ \left(\mathcal{L}_\Gamma e_{p_n,l}^i + e_{g_n,l}^i, \psi_{n,l}\right)_\Gamma = 0, \tag{4.11}$$
$$\phi_l\left(\tfrac{e_{s,l}^i}{\Delta t}, \psi_{w,l}\right)_{\Omega_l} - \mathcal{L}_{p,l}\left(e_{p_c,l}^i - e_{p_c,l}^{i-1}, \psi_{w,l}\right)_{\Omega_l} - \left(\mathbf{u}_{w,l}^{k,\theta,i} - \mathbf{u}_{w,l}^{k,\theta}, \nabla\psi_{w,l}\right)_{\Omega_l}$$
$$+ \left(\mathcal{L}_\Gamma e_{p_w,l}^i + e_{g_w,l}^i, \psi_{w,l}\right)_\Gamma = 0, \tag{4.12}$$
$$e_{g_\alpha,l}^i = -2\mathcal{L}_\Gamma e_{p_\alpha,3-l}^{i-1} - e_{g_\alpha,3-l}^{i-1} \quad \text{in } L^2(\Gamma), \tag{4.13}$$
$$\tfrac{e_{s,l}^i}{\Delta t} = \theta(\Psi_l^{k,i} - \Psi_l^k) \quad \text{in } L^2(\Omega_l). \tag{4.14}$$

Error estimate on the saturation. Equation (4.14) yields

$$\begin{aligned}\tfrac{1}{\Delta t}\left\|e_{s,l}^i\right\|_{\Omega_l} &= \theta\left\|\Psi_l^{k,i} - \Psi_l^k\right\|_{\Omega_l}\\ &\leq \theta\left\|\Psi_l^{k,i} - \Psi_l(p_{n,l}^k - p_{w,l}^k - p_{c,l}(s_l^{k,i}))\right\|_{\Omega_l} + \theta\left\|\Psi_l(p_{n,l}^k - p_{w,l}^k - p_{c,l}(s_l^{k,i})) - \Psi_l^k\right\|_{\Omega_l}\\ &\leq \theta\left\|e_{\Psi,l}^i\right\|_{\Omega_l} + \theta L_{\Psi,l}L_{p_c,l}\left\|e_{s_l}^i\right\|.\end{aligned}$$

In the last step, the Lipschitz continuity of Ψ_l and $p_{c,l}$ was used. Multiplying by Δt and using $\Delta t \leq (2\theta L_{\Psi,l}L_{p_c,l})^{-1}$ yields

$$\left\|e_{s,l}^i\right\|_{\Omega_l} \leq 2\theta\Delta t\left\|e_{\Psi,l}^i\right\|_{\Omega_l}. \tag{4.15}$$

Error estimate on the non-wetting pressure. Note that (4.13) again leads to (4.6). Therefore, testing (4.11) with $\psi_{n,l} = e^i_{p_n,l}$ yields

$$-\phi_l\left(\tfrac{e^i_{s,l}}{\Delta t},\, e^i_{p_n,l}\right)_{\Omega_l} + \mathcal{L}_{p,l}\left(e^i_{p_c,l} - e^{i-1}_{p_c,l},\, e^i_{p_n,l}\right)_{\Omega_l} + \theta\left(\lambda_{n,l}(s^{k,i}_l)K_l\nabla e^i_{p_n,l},\, \nabla e^i_{p_n,l}\right)_{\Omega_l}$$
$$= -\theta\left((\lambda_{n,l}(s^{k,i}_l) - \lambda_{n,l}(s^k_l))K_l\nabla p^k_{n,l},\, \nabla e^i_{p_n,l}\right)_{\Omega_l} + \tfrac{1}{4\mathcal{L}_\Gamma}\left(\left\|e^{i+1}_{g_n,l}\right\|^2_\Gamma - \left\|e^i_{g_n,3-l}\right\|^2_\Gamma\right).$$

By the lower bound $m_{\lambda_n,l}$ on $\lambda_{n,l}$, the Lipschitz continuity of $\lambda_{n,l}$ and the bound on the pressure gradient, one obtains with the Cauchy-Schwarz inequality

$$-\phi_l\left(\tfrac{e^i_{s,l}}{\Delta t},\, e^i_{p_n,l}\right)_{\Omega_l} + \mathcal{L}_{p,l}\left(e^i_{p_c,l} - e^{i-1}_{p_c,l},\, e^i_{p_n,l}\right)_{\Omega_l} + \theta m_{\lambda_n,l}\left\|K_l^{1/2}\nabla e^i_{p_n,l}\right\|^2_{\Omega_l}$$
$$\le \theta L_{\lambda_n,l}M_{p_n,l}\left\|e^i_{s,l}\right\|_{\Omega_l}\left\|K^{1/2}\nabla e^i_{p_n,l}\right\|_{\Omega_l} + \tfrac{1}{4\mathcal{L}_\Gamma}\left(\left\|e^{i+1}_{g_n,l}\right\|^2_\Gamma - \left\|e^i_{g_n,3-l}\right\|^2_\Gamma\right).$$

Young's inequality and estimate (4.15) lead to

$$-\phi_l\left(\tfrac{e^i_{s,l}}{\Delta t},\, e^i_{p_n,l}\right)_{\Omega_l} + \mathcal{L}_{p,l}\left(e^i_{p_c,l} - e^{i-1}_{p_c,l},\, e^i_{p_n,l}\right)_{\Omega_l} + \tfrac{\theta m_{\lambda_n,l}}{2}\left\|K_l^{1/2}\nabla e^i_{p_n,l}\right\|^2_{\Omega_l}$$
$$\le \tfrac{2\Delta t^2\theta^3 L^2_{\lambda_n,l}M^2_{p_n,l}}{m_{\lambda_n,l}}\left\|e^i_{\Psi,l}\right\|^2_{\Omega_l} + \tfrac{1}{4\mathcal{L}_\Gamma}\left(\left\|e^{i+1}_{g_n,l}\right\|^2_\Gamma - \left\|e^i_{g_n,3-l}\right\|^2_\Gamma\right). \tag{4.16}$$

Error estimate on the wetting pressure. Testing (4.3) with $\psi_{w,l} = e^i_{p_w,l}$ and following the same steps as for the non-wetting pressure equation yields

$$\phi_l\left(\tfrac{e^i_{s,l}}{\Delta t},\, e^i_{p_w,l}\right)_{\Omega_l} - \mathcal{L}_{p,l}\left(e^i_{p_c,l} - e^{i-1}_{p_c,l},\, e^i_{p_w,l}\right)_{\Omega_l} + \tfrac{\theta m_{\lambda_w,l}}{2}\left\|K_l^{1/2}\nabla e^i_{p_w,l}\right\|^2_{\Omega_l}$$
$$\le \tfrac{2\Delta t^2\theta^3 L^2_{\lambda_w,l}M^2_{p_w,l}}{m_{\lambda_w,l}}\left\|e^i_{\Psi,l}\right\|^2_{\Omega_l} + \tfrac{1}{4\mathcal{L}_\Gamma}\left(\left\|e^i_{g_w,l}\right\|^2_\Gamma - \left\|e^{i+1}_{g_w,3-l}\right\|^2_\Gamma\right). \tag{4.17}$$

Combined error estimate. Addition of the pressure estimates (4.16) and (4.17) yields by the identity $(a-b)a = \frac{1}{2}(a^2 - b^2 + (a-b)^2)$

$$-\phi_l\left(\tfrac{e^i_{s,l}}{\Delta t},\, e^i_{p_c,l}\right)_{\Omega_l} + \tfrac{\mathcal{L}_{p,l}}{2}\left(\left\|e^i_{p_c,l}\right\|^2_{\Omega_l} - \left\|e^{i-1}_{p_c,l}\right\|^2_{\Omega_l} + \left\|e^i_{p_c,l} - e^{i-1}_{p_c,l}\right\|^2_{\Omega_l}\right)$$
$$+ \sum_{\alpha\in\{n,w\}}\tfrac{\theta m_{\lambda_\alpha,l}}{2}\left\|K_l^{1/2}\nabla e^i_{p_\alpha,l}\right\|^2_{\Omega_l}$$
$$\le \tfrac{1}{4\mathcal{L}_\Gamma}\sum_{\alpha\in\{n,w\}}\left(\left\|e^i_{g_\alpha,l}\right\|^2_\Gamma - \left\|e^{i+1}_{g_\alpha,3-l}\right\|^2_\Gamma\right) + \sum_{\alpha\in\{n,w\}}\tfrac{2\Delta t^2\theta^3 L^2_{\lambda_\alpha,l}M^2_{p_\alpha,l}}{m_{\lambda_\alpha,l}}\left\|e^i_{\Psi,l}\right\|^2_{\Omega_l}. \tag{4.18}$$

The first term on the lefthand side can be estimated as follows. Using (4.14) and $\Psi^* := \Psi_l(p^k_{n,l} - p^k_{w,l} - p_{c,l}(s^{k,i}_l))$, one obtains

$$\left(\tfrac{e^i_{s,l}}{\Delta t},\, e^i_{p_c,l}\right)_{\Omega_l} = \left(\tfrac{e^i_{s,l}}{\Delta t},\, e^i_{p_c,l} - e^{i-1}_{p_c,l}\right)_{\Omega_l} + \theta\left(\Psi^{k,i}_l - \Psi^* + \Psi^* - \Psi^k_l,\, e^{i-1}_{p_c,l}\right)_{\Omega_l}$$
$$\le \tfrac{1}{\Delta t}\left\|e^i_{s,l}\right\|_{\Omega_l}\left\|e^i_{p_c,l} - e^{i-1}_{p_c,l}\right\|_{\Omega_l} + \theta\left(e^i_{\Psi,l},\, e^{i-1}_{p_c,l}\right)_{\Omega_l}$$
$$+ \theta\left(\Psi_l\left(p^k_{n,l} - p^k_{w,l} - p_{c,l}(s^{k,i}_l)\right) - \Psi_l\left(p^k_{n,l} - p^k_{w,l} - p_{c,l}(s^k_l)\right),\, e^{i-1}_{p_c,l}\right)_{\Omega_l}.$$

Since Ψ_l, $p_{c,l}$ are decreasing and Lipschitz-continuous, one gets

$$\left(\tfrac{e^i_{s,l}}{\Delta t},\ e^i_{p_c,l}\right)_{\Omega_l} \leq \tfrac{1}{\Delta t}\left\|e^i_{s,l}\right\|_{\Omega_l}\left\|e^i_{p_c,l}-e^{i-1}_{p_c,l}\right\|_{\Omega_l} - \tfrac{\theta}{L_{\Psi,l}}\left\|e^i_{\Psi,l}\right\|^2_{\Omega_l} + \theta L_{\Psi,l}L_{p_c,l}\left\|e^i_{s_l}\right\|_{\Omega_l}\sum_{\alpha\in\{n,w\}}\left\|e^{i-1}_{p_\alpha,l}\right\|_{\Omega_l}.$$

With the estimate (4.15), Young's inequality yields for $\epsilon_\alpha > 0$

$$\left(\tfrac{e^i_{s,l}}{\Delta t},\ e^i_{p_c,l}\right)_{\Omega_l} \leq \Big(\tfrac{2\phi_l\theta^2}{\mathcal{L}_{p,l}} + \sum_{\alpha\in\{n,w\}}\tfrac{\Delta t^2\theta^4 L^2_{\Psi,l}L^2_{p_c,l}}{\epsilon_\alpha} - \tfrac{\theta}{L_{\Psi,l}}\Big)\left\|e^i_{\Psi,l}\right\|^2_{\Omega_l} + \tfrac{\mathcal{L}_{p,l}}{2\phi_l}\left\|e^i_{p_c,l}-e^{i-1}_{p_c,l}\right\|^2_{\Omega_l} + \sum_{\alpha\in\{n,w\}}\epsilon_\alpha\left\|e^{i-1}_{p_\alpha,l}\right\|^2_{\Omega_l}.$$

The Poincaré inequality (with C_{Ω_l} the domain dependent constant) leads to

$$\left(\tfrac{e^i_{s,l}}{\Delta t},\ e^i_{p_c,l}\right)_{\Omega_l} \leq \Big(\tfrac{2\phi_l\theta^2}{\mathcal{L}_{p,l}} + \sum_{\alpha\in\{n,w\}}\tfrac{\Delta t^2\theta^4 L^2_{\Psi,l}L^2_{p_c,l}}{\epsilon_\alpha} - \tfrac{\theta}{L_{\Psi,l}}\Big)\left\|e^i_{\Psi,l}\right\|^2_{\Omega_l} + \tfrac{\mathcal{L}_{p,l}}{2\phi_l}\left\|e^i_{p_c,l}-e^{i-1}_{p_c,l}\right\|^2_{\Omega_l} + \sum_{\alpha\in\{n,w\}}\tfrac{\epsilon_\alpha C^2_{\Omega_l}}{\underline{K}_l}\left\|K_l^{1/2}\nabla e^{i-1}_{p_\alpha,l}\right\|^2_{\Omega_l}.$$

Multiplying this estimate by ϕ_l, choosing $\epsilon_\alpha = \theta m_{\lambda_\alpha,l}\underline{K}_l(4\phi_l C^2_{\Omega_l})^{-1}$, and adding to (4.18), one is left with

$$\tfrac{\mathcal{L}_{p,l}}{2}\left(\left\|e^i_{p_c,l}\right\|^2_{\Omega_l} - \left\|e^{i-1}_{p_c,l}\right\|^2_{\Omega_l}\right) + \sum_{\alpha\in\{n,w\}}\tfrac{\theta m_{\lambda_\alpha,l}}{2}\left\|K_l^{1/2}\nabla e^i_{p_\alpha,l}\right\|^2_{\Omega_l} + C_l(\Delta t)\left\|e^i_{\Psi,l}\right\|^2_{\Omega_l} \leq \tfrac{1}{4\mathcal{L}_\Gamma}\sum_{\alpha\in\{n,w\}}\left(\left\|e^i_{g_\alpha,l}\right\|^2_\Gamma - \left\|e^{i+1}_{g_\alpha,3-l}\right\|^2_\Gamma\right) + \sum_{\alpha\in\{n,w\}}\tfrac{\theta m_{\lambda_\alpha,l}}{4}\left\|K_l^{1/2}\nabla e^{i-1}_{p_\alpha,l}\right\|^2_{\Omega_l},$$

where

$$C_l(\Delta t) = \tfrac{\phi_l\theta}{L_{\Psi,l}} - \tfrac{2\phi_l^2\theta^2}{\mathcal{L}_{p,l}} - \Delta t^2\sum_{\alpha\in\{n,w\}}\left(\tfrac{4\phi_l^2\theta^3 L^2_{\Psi,l}L^2_{p_c,l}C^2_{\Omega_l}}{m_{\lambda_\alpha,l}\underline{K}_l} + \tfrac{2\theta^3 L^2_{\lambda_\alpha,l}M^2_{p_\alpha,l}}{m_{\lambda_\alpha,l}}\right).$$

By assumption, $\mathcal{L}_{p,l} > 2\phi_l\theta L_{\Psi,l}$ and Δt is small enough, such that $C_l(\Delta t) \geq 0$. Then, summation of the estimates for $l \in \{1,2\}$ and $i = 1,2,\dots,r$ yields

$$\sum_{i=1}^r\sum_{l=1}^2\sum_{\alpha\in\{n,w\}}\tfrac{\theta m_{\lambda_\alpha,l}}{4}\left\|K_l^{1/2}\nabla e^i_{p_\alpha,l}\right\|^2_{\Omega_l} + \sum_{i=1}^r\sum_{l=1}^2 C_l(\Delta t)\left\|e^i_{\Psi,l}\right\|^2_{\Omega_l} \leq \tfrac{1}{4\mathcal{L}_\Gamma}\sum_{l=1}^2\sum_{\alpha\in\{n,w\}}\left\|e^1_{g_\alpha,l}\right\|^2_\Gamma + \sum_{l=1}^2\tfrac{\mathcal{L}_{p,l}}{2}\left\|e^0_{p_c,l}\right\|^2_{\Omega_l} + \sum_{l=1}^2\sum_{\alpha\in\{n,w\}}\tfrac{\theta m_{\lambda_\alpha,l}}{4}\left\|K_l^{1/2}\nabla e^0_{p_\alpha,l}\right\|^2_{\Omega_l}.$$

Since the righthand side is independent of r, we conclude that the series on the left is absolutely convergent. By the Poincaré inequality and estimate (4.15), we conclude $p^{k,i}_{\alpha,l} \to p^k_{\alpha,l}$ in $\mathcal{W}_l$ and $s^{k,i}_l \to s^k_l$ in $L^2(\Omega_l)$. The weak convergence $e^i_{g_\alpha,l} \rightharpoonup 0$ in $L^2(\Gamma)$ can be shown exactly as in Theorem 4.1 by the limit $i \to \infty$ in (4.11) and (4.12). □

5. Numerical Experiments

For the numerical validation of the theoretical results above, we present several numerical studies in two spatial dimensions. We focus on three aspects: the convergence behavior in space and time of the whole method, the convergence behavior of the LDD-schemes within single time steps, and the choice of the parameters. Three examples with manufactured solution are presented, followed by a realistic application.

The theoretical results above are independent of the spatial discretization. For Richards' equation and two-phase flow models with equilibrium capillary pressure as well as dynamic capillarity, the (mixed) finite element method was used in [2–4], the discontinuous Galerkin method in [5, 61] and the finite volume method in [6, 62–64]. General gradient schemes were considered in [59, 65]. Since the pressure equations are elliptic, we choose here a standard finite element method (Q_2) on a uniform, rectangular mesh of width Δx matching at the interface Γ. We use the Crank-Nicolson method ($\theta = 1/2$) in time, so that errors of order $O(\Delta t^2 + \Delta x^2)$ are expected for sufficiently smooth solutions. At each time step, the LDD-schemes are stopped, when the relative L^2-norm of the difference of subsequent iterative solutions drops below 10^{-8}. To obtain the implicitly given saturation in the LDD-scheme II, the fixed-point iteration discussed in the proof of Lemma 4.2 is used up to a residual of 10^{-12}. For simplicity, we take the same linearization parameters on both subdomains, i.e. $\mathcal{L}_a := \mathcal{L}_{a,1} = \mathcal{L}_{a,2}$ for $a \in \{p, T, \Phi\}$.

The implementation was done in `C++` using the library `deal.II` [66]. All calculations were performed on a Linux octa-core system.

5.1. Analytic Test Cases

For the three examples with manufactured solution, one can explicitly compute the errors and thereby the experimental order of convergence (EOC). For simplicity, we assume an isotropic and constant absolute permeability on the whole domain, i.e. $K_1 = K_2 = 1$, and a constant porosity $\phi_1 = \phi_2 = 1$. We set the final time $T = 1$, and decomposed the domain $\Omega = (-1, 1) \times (0, 1)$ at the interface $\Gamma = \{0\} \times (0, 1)$ into $\Omega_1 = (-1, 0) \times (0, 1)$ and $\Omega_2 = (0, 1) \times (0, 1)$.

5.1.1. Linear Coefficient Functions Without Hysteresis

We consider a simple nonlinear problem with linear coefficient functions, but no hysteresis. These functions are therefore chosen

$$\lambda_n(s) = 1 - s, \qquad \lambda_w(s) = s, \qquad p_c(s) = 0.2 - s, \qquad \tau \equiv 1, \qquad \gamma \equiv 0.$$

The righthand side terms are selected such that the analytic solution is given by

$$p_n(\mathbf{x}, t) = \tfrac{(1-x_1)(1+x_1)^2}{2(1+t)^2}, \qquad p_w(\mathbf{x}, t) = \tfrac{(1-x_1)(1+x_1)^2}{2(1+t)}, \qquad s(\mathbf{x}, t) = \tfrac{(1-x_1)(1+x_1)^2}{2(1+t)} + 0.2.$$

This corresponds to homogeneous Dirichlet boundary conditions at $x_1 = \pm 1$, homogeneous Neumann boundary conditions at $x_2 \in \{0, 1\}$. Note that in this special case, the two schemes almost coincide, since they only differ in the inverted capillary pressure equation, which is a linear transformation here, and thus the results are very similar.

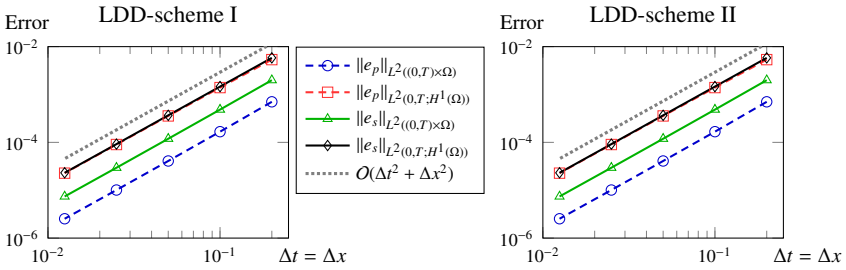

Figure 2: Second order convergence in time step size Δt and mesh width Δx of pressure and saturation is observed for both LDD-schemes in the case with linear coefficients, but no hysteresis.

Δt	Δx	$\|e_p\|_{L^2(0,T;H^1(\Omega))}$	EOC$_p$	$\|e_s\|_{L^2(0,T;H^1(\Omega))}$	EOC$_s$	Avg.-Iter.
0.2	0.2	$5.352 \cdot 10^{-3}$		$5.824 \cdot 10^{-3}$		13
0.1	0.1	$1.394 \cdot 10^{-3}$	1.94	$1.463 \cdot 10^{-3}$	1.993	12.3
0.05	0.05	$3.564 \cdot 10^{-4}$	1.968	$3.670 \cdot 10^{-4}$	1.995	12
0.025	0.025	$9.013 \cdot 10^{-5}$	1.983	$9.192 \cdot 10^{-5}$	1.997	11.5
0.0125	0.0125	$2.273 \cdot 10^{-5}$	1.987	$2.312 \cdot 10^{-5}$	1.991	15.5

Table 1: Convergence study and average number of LDD-iterations per time step of the LDD-scheme I for varying time step size Δt and mesh width Δx in the case with linear coefficients, but no hysteresis.

Δt	Δx	$\|e_p\|_{L^2(0,T;H^1(\Omega))}$	EOC$_p$	$\|e_s\|_{L^2(0,T;H^1(\Omega))}$	EOC$_s$	Avg.-Iter.
0.2	0.2	$5.352 \cdot 10^{-3}$		$5.824 \cdot 10^{-3}$		13
0.1	0.1	$1.394 \cdot 10^{-3}$	1.94	$1.463 \cdot 10^{-3}$	1.993	12
0.05	0.05	$3.564 \cdot 10^{-4}$	1.968	$3.670 \cdot 10^{-4}$	1.995	12
0.025	0.025	$9.013 \cdot 10^{-5}$	1.983	$9.192 \cdot 10^{-5}$	1.997	11.3
0.0125	0.0125	$2.273 \cdot 10^{-5}$	1.987	$2.312 \cdot 10^{-5}$	1.991	16.2

Table 2: Convergence study and average number of LDD-iterations per time step of the LDD-scheme II for varying time step size Δt and mesh width Δx in the case with linear coefficients, but no hysteresis.

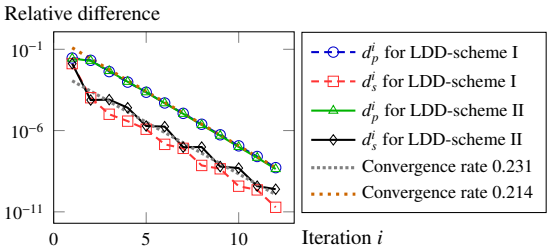

Figure 3: The LDD-schemes converge very fast and linearly in the last time step of the case with linear coefficient functions, but no hysteresis. Plotted are the relative differences of pressure and saturation between consecutive iterations, together with the fitted convergence rates.

First, we study the convergence order of the two methods with respect to the time step size Δt and the mesh width Δx. For the LDD-scheme I, the parameters are $\mathcal{L}_p = 0.5$, $\mathcal{L}_T = 1$ and $\mathcal{L}_\Gamma = 0.375$ ($\mathcal{L}_\Phi = 0$), while for the LDD-scheme II, the parameters are $\mathcal{L}_p = 0.5$ and $\mathcal{L}_\Gamma = 0.375$. Second order convergence of pressure and saturation is observed for both schemes, as clearly shown in Tables 1 and 2 and Fig. 2. This even holds for the saturation in the $L^2(0,T;H^1(\Omega))$ norm, which is not covered by the above theoretical results.

With decreasing time step size Δt, the average iteration number per time step and thus the convergence rate stay almost constant. This result is surprising, since the convergence rate asymptotically deteriorates for both, the L-scheme and the domain decomposition method. For L-schemes, the converge rate typically is $\sqrt{C/(C+\Delta t)}$ for some $C > 0$ (see e.g. [2, 4]), and for the domain decomposition method with optimal parameter, one obtains convergence rates of $1 - O(\sqrt{\Delta t})$ (see e.g. [14, 16]). Here, the pre-asymptotic regime leads to the different behavior, which seems to end around $\Delta t = 0.025$.

Moreover, the analysis provides convergence independently of the initial guess. This could also be observed, when the initial guess in each time step was fixed to $p_n^{k,0} = p_w^{k,0} \equiv 1$ and $s^{k,0} \equiv 0.75$ for the above simulations with $\Delta t = \Delta x = 0.05$. In this case, the resulting errors $\|e_p\|_{L^2(0,T;H^1(\Omega))}$ and $\|e_s\|_{L^2(0,T;H^1(\Omega))}$ were the same as in the studies above ($\pm 0.1\%$), only the average number of LDD-iterations per time step increased by about 20%.

Next, the convergence properties within one time step are considered. Therefore, the relative differences in pressure and saturation between consecutive iterations

$$d_p^i := \sqrt{\left\| \frac{p_n^{k,i} - p_n^{k,i-1}}{p_n^{k,i}} \right\|_{L^2(\Omega)}^2 + \left\| \frac{p_w^{k,i} - p_w^{k,i-1}}{p_w^{k,i}} \right\|_{L^2(\Omega)}^2}, \qquad d_s^i := \left\| \frac{s^{k,i} - s^{k,i-1}}{s^{k,i}} \right\|_{L^2(\Omega)},$$

are plotted in Fig. 3 for the last time step of the above simulations with $\Delta t = \Delta x = 0.05$. These results indicate a very fast, linear convergence. This fast convergence depends on a proper choice of the parameters. The average number of LDD-iterations per time step is minimal for a specific set of parameters and increases drastically for small deviations from that (see Fig. 4). The linearization parameters typically should be chosen as small as possible, but big enough to ensure convergence (see e.g. [2, 4, 22]). Here,

that means that lower bounds from our analysis (see Theorems 4.1 and 4.2) should be good predictions. They are $\mathcal{L}_p \geq 1/2$ and $\mathcal{L}_T \geq 1/2$ for the first scheme and $\mathcal{L}_p > 1$ for the second one, and are indeed very close to the optimal ones. On the other hand, theoretical prediction of the domain decomposition parameter $\mathcal{L}_\Gamma$ is usually based on the Fourier transformation [14, 16, 18], which cannot be directly applied to nonlinear problems. Therefore, there are no such predictions available yet for this type of nonlinear equations.

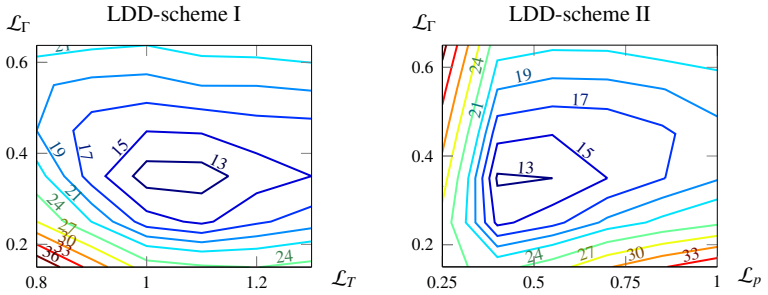

Figure 4: Parameter dependence of the average number of LDD-iterations per time step for $\Delta t = \Delta x = 0.05$ in the case with linear coefficients, but no hysteresis. For simplicity, $\mathcal{L}_p = 0$ for LDD-scheme I.

5.1.2. Nonlinear Coefficient Functions Without Hysteresis

Next, we consider a problem with nonlinear coefficient functions, again excluding hysteresis. These functions are

$$\lambda_n(s) = (1-s)^2, \qquad \lambda_w(s) = s^2, \qquad p_c(s) = -s^2, \qquad \tau(s) = s, \qquad \gamma \equiv 0.$$

The righthand sides are chosen in such a way that the analytic solution is given by

$$p_n(\mathbf{x},t) = 1 - \tfrac{(3-2t)(3+2(x_2-x_1))^2}{400}, \qquad p_w(\mathbf{x},t) = 1 + \tfrac{(3-2t)(3+2(x_2-x_1))^2}{400},$$
$$s(\mathbf{x},t) = \tfrac{(3+2(x_2-x_1))\sqrt{1+t}}{10},$$

where the corresponding boundary conditions are for simplicity the given exact values, i.e. inhomogeneous Dirichlet values on the whole boundary $\partial\Omega$. Note, that the solutions are polynomials of degree two, and thus the spatial discretization (Q_2) is exact, so that the mesh width $\Delta x = 0.05$ is fixed in the following. The parameters were $\mathcal{L}_p = 0.5$, $\mathcal{L}_T = 0.55$ and $\mathcal{L}_\Gamma = 2.65$ ($\mathcal{L}_\Phi = 0$) for the LDD-scheme I, while $\mathcal{L}_p = 1.5$ and $\mathcal{L}_\Gamma = 2.65$ for the LDD-scheme II.

As before, second order convergence in Δt is achieved by both schemes, again even for the saturation in the $L^2(0,T;H^1(\Omega))$ norm (see Fig. 5 and Tables 3 and 4). The average number of LDD-iterations per time step is two times bigger than in the previous example due to the stronger nonlinearities. This time, it even decreases for decreasing time step size Δt, which indicates here an early pre-asymptotic regime, where the smaller differences between solutions of consecutive time steps lead to a smaller number of necessary iterations. Fixing the initial guess ($s \equiv 0.25$ and $p_n =$

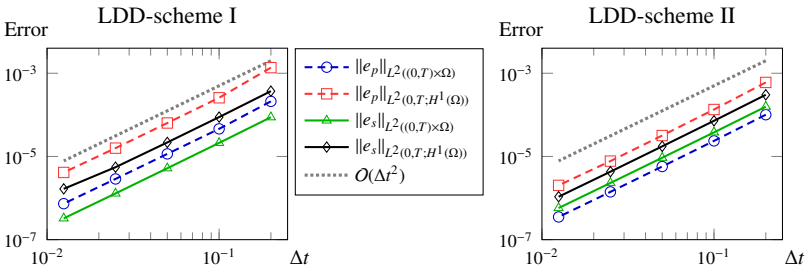

Figure 5: Second order convergence in the time step size Δt of pressure and saturation is observed for both LDD-schemes in the case with nonlinear coefficients, but no hysteresis.

Δt	$\|e_p\|_{L^2(0,T;H^1(\Omega))}$	EOC$_p$	$\|e_s\|_{L^2(0,T;H^1(\Omega))}$	EOC$_s$	Avg.-Iter.
0.2	$1.363 \cdot 10^{-3}$		$3.712 \cdot 10^{-4}$		51.8
0.1	$2.573 \cdot 10^{-4}$	2.405	$8.829 \cdot 10^{-5}$	2.072	46.6
0.05	$6.370 \cdot 10^{-5}$	2.014	$2.174 \cdot 10^{-5}$	2.022	43.2
0.025	$1.584 \cdot 10^{-5}$	2.007	$5.519 \cdot 10^{-6}$	1.978	41.6
0.0125	$4.126 \cdot 10^{-6}$	1.941	$1.665 \cdot 10^{-6}$	1.729	41.1

Table 3: Convergence study and average number of LDD-iterations per time step of the LDD-scheme I for varying time step size Δt in the case with nonlinear coefficients, but no hysteresis.

Δt	$\|e_p\|_{L^2(0,T;H^1(\Omega))}$	EOC$_p$	$\|e_s\|_{L^2(0,T;H^1(\Omega))}$	EOC$_s$	Avg.-Iter.
0.2	$6.017 \cdot 10^{-4}$		$3.036 \cdot 10^{-4}$		49.6
0.1	$1.345 \cdot 10^{-4}$	2.162	$7.200 \cdot 10^{-5}$	2.076	44.5
0.05	$3.181 \cdot 10^{-5}$	2.08	$1.750 \cdot 10^{-5}$	2.04	40.1
0.025	$7.733 \cdot 10^{-6}$	2.04	$4.305 \cdot 10^{-6}$	2.023	36.6
0.0125	$2.020 \cdot 10^{-6}$	1.937	$1.076 \cdot 10^{-6}$	2	33.6

Table 4: Convergence study and average number of LDD-iterations per time step of the LDD-scheme II for varying time step size Δt in the case with nonlinear coefficients, but no hysteresis.

$p_w \equiv 2$) resulted in the same errors $\|e_p\|_{L^2(0,T;H^1(\Omega))}$ and $\|e_s\|_{L^2(0,T;H^1(\Omega))}$ ($\pm 0.3\%$) as in the above studies with $\Delta t = 0.05$, but a significantly increased number of iterations per time step (71% and 89% for LDD-scheme I and II, respectively).

Next, the convergence properties of the methods within one time step are discussed. In the last time step of the above simulations with $\Delta t = 0.05$, we observed again a fast and almost linear convergence (see Fig. 6). The parameter dependence of the average number of iterations per time step shows a different behavior in this case (see Fig. 7). Only the second scheme has an optimal parameter set, whereas the first one shows improving convergence for decreasing $\mathcal{L}_T \to 0.6$ until it suddenly does not converge any more. The latter agrees very well with the theory, which predicts $\mathcal{L}_p \geq 1$ and $\mathcal{L}_T \geq 1/2$ for the LDD-scheme I, while $\mathcal{L}_p > 1$ for the second one is again very close to the optimum at 1.5. Furthermore, small deviations from the optima have less impact than in the previous example.

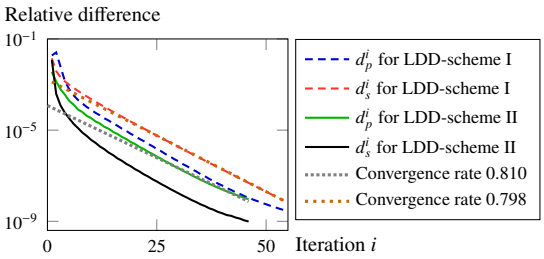

Figure 6: The LDD-schemes converge fast and almost linearly in the last time step of the case with nonlinear coefficient functions, but no hysteresis. Plotted are the relative differences of pressure and saturation between consecutive iterations, together with the fitted convergence rates.

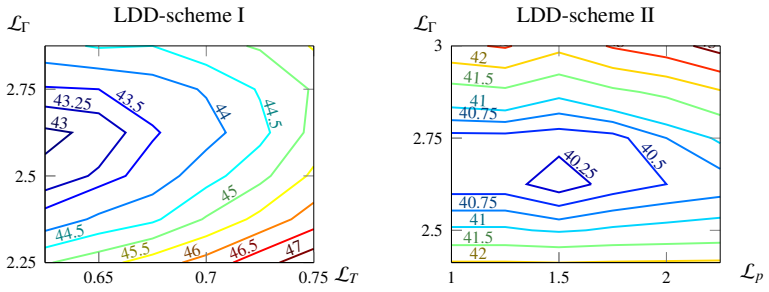

Figure 7: Parameter dependence of the average number of LDD-iterations per time step for $\Delta t = 0.05$ in the case with nonlinear coefficients, but no hysteresis. For simplicity, $\mathcal{L}_p = 0$ for LDD-scheme I.

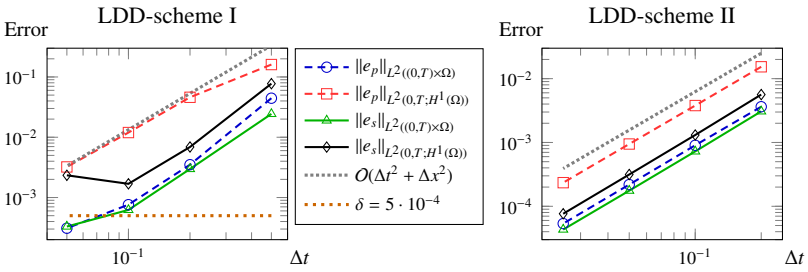

Figure 8: Second order convergence in time step size Δt and mesh width Δx of pressure and saturation is observed for both LDD-schemes in the case with linear coefficients, including hysteresis. The mesh width is $\Delta x = \Delta t/2$ for LDD-scheme I and $\Delta x = \Delta t/4$ for LDD-scheme II.

5.1.3. Linear Coefficient Functions Including Hysteresis

Finally, we consider a problem including hysteresis, where the linear coefficient functions are

$$\lambda_n(s) = 1 - s, \qquad \lambda_w(s) = s, \qquad p_c(s) = -s, \qquad \tau \equiv 1, \qquad \gamma \equiv 1.$$

Since hysteresis occurs during the change between imbibition and drainage, we constructed righthand side terms which yield the following manufactured solution

$$s(\mathbf{x},t) = \begin{cases} \frac{1}{2}\cos\left((t_0(\mathbf{x}) - t)^2\right) & \text{if } t < t_0(\mathbf{x}), \\ \frac{1}{2} & \text{if } t_0(\mathbf{x}) \le t \le t_1(\mathbf{x}), \\ \frac{1}{2}\cos\left((t - t_1(\mathbf{x}))^2\right) & \text{if } t_1(\mathbf{x}) < t, \end{cases}$$

$$p_n(\mathbf{x},t) = \begin{cases} 1 - \frac{1}{2}\cos\left((t_0(\mathbf{x}) - t)^2\right) & \text{if } t < t_0(\mathbf{x}), \\ 6\xi^5(t,\mathbf{x}) - 15\xi^4(t,\mathbf{x}) + 10\xi^3(t,\mathbf{x}) + \frac{1}{2} & \text{if } t_0(\mathbf{x}) \le t \le t_1(\mathbf{x}), \\ 2 - \frac{1}{2}\cos((t - t_1(\mathbf{x}))^2) & \text{if } t_1(\mathbf{x}) < t, \end{cases}$$

$$p_w(\mathbf{x},t) = \begin{cases} 2 + \sqrt{(t_0(\mathbf{x}) - t)^2}\sin\left((t_0(\mathbf{x}) - t)^2\right) & \text{if } t < t_0(\mathbf{x}), \\ -6\xi^5(t,\mathbf{x}) + 15\xi^4(t,\mathbf{x}) - 10\xi^3(t,\mathbf{x}) + 2 & \text{if } t_0(\mathbf{x}) \le t \le t_1(\mathbf{x}), \\ 1 - \sqrt{(t - t_1(\mathbf{x}))^2}\sin((t - t_1(\mathbf{x}))^2) & \text{if } t_1(\mathbf{x}) < t, \end{cases}$$

where

$$t_0(\mathbf{x}) := \tfrac{10x_1+7}{20}, \quad t_1(\mathbf{x}) := t_0(\mathbf{x}) + \tfrac{3}{10} = \tfrac{10x_1+13}{20}, \quad \xi(t,\mathbf{x}) := \tfrac{t - t_0(\mathbf{x})}{t_1(\mathbf{x}) - t_0(\mathbf{x})}.$$

The corresponding boundary conditions are simply chosen to be of inhomogeneous Dirichlet type at $x_1 = \pm 1$, and of homogeneous Neumann type at $x_2 \in \{0, 1\}$. For the LDD-scheme I, the regularization parameter is chosen $\delta = 5 \cdot 10^{-4}$ and the LDD parameters are $\mathcal{L}_p = 0.5$, $\mathcal{L}_T = 2$, $\mathcal{L}_\Phi = 10^3$ and $\mathcal{L}_\Gamma = 0.375$. In this case, we used a reduced stopping criterion for the LDD-scheme of 10^{-7}. For the LDD-scheme II, the parameters are $\mathcal{L}_p = 0.33$ and $\mathcal{L}_\Gamma = 0.375$.

As before, second order convergence with respect to the time step size Δt and mesh width Δx is observed for both schemes, until the errors due to regularization are dominating in the first scheme (see Tables 5 and 6 and Fig. 8). Here, the inverted formulation

Δt	Δx	$\|e_p\|_{L^2(0,T;H^1(\Omega))}$	EOC$_p$	$\|e_s\|_{L^2(0,T;H^1(\Omega))}$	EOC$_s$	Avg.-Iter.
0.5	0.25	0.161		$7.739 \cdot 10^{-2}$		5,525
0.2	0.1	$4.600 \cdot 10^{-2}$	1.364	$6.891 \cdot 10^{-3}$	2.64	4,890
0.1	0.05	$1.196 \cdot 10^{-2}$	1.943	$1.688 \cdot 10^{-3}$	2.029	4,380
0.05	0.025	$3.215 \cdot 10^{-3}$	1.895	$2.336 \cdot 10^{-3}$	−0.469	3,900

Table 5: Convergence study and average number of LDD-iterations per time step of the LDD-scheme I for varying time step in the full analytical case with linear coefficients including hysteresis.

Δt	Δx	$\|e_p\|_{L^2(0,T;H^1(\Omega))}$	EOC$_p$	$\|e_s\|_{L^2(0,T;H^1(\Omega))}$	EOC$_s$	Avg.-Iter.
0.2	0.05	$1.534 \cdot 10^{-2}$		$5.631 \cdot 10^{-3}$		17.8
0.1	0.025	$3.788 \cdot 10^{-3}$	2.018	$1.309 \cdot 10^{-3}$	2.105	17
0.05	0.0125	$9.454 \cdot 10^{-4}$	2.002	$3.147 \cdot 10^{-4}$	2.056	16.5
0.025	0.0063	$2.345 \cdot 10^{-4}$	2.011	$7.640 \cdot 10^{-5}$	2.042	15.6

Table 6: Convergence study and average number of LDD-iterations per time step of the LDD-scheme II for varying time step in the full analytical case with linear coefficients including hysteresis.

of the second scheme is clearly advantageous. While the first scheme needs a huge parameter $\mathcal{L}_\Phi$ for a moderate regularization parameter δ due to the steep slope in the capillary pressure equation near zero, the second scheme has no such restriction due to the inverted formulation. Therefore, the average number of iterations per time step for the LDD-scheme I is huge, which makes this scheme unpractical for such problems. In contrast, the average number of iteration for the LDD-scheme II is very low, which again shows that the latter is the preferable method for this type of applications. As before, we observe the iteration number to decrease for decreasing time step size due to the pre-asymptotic regime. Furthermore, if the initial guess is fixed to $s^{k,0} \equiv 0.75$ and $p_n^{k,0} = p_w^{k,0} \equiv 1$ in each time step, the errors are similar to those in the original studies with $\Delta t = 0.1$, (+35% for LDD-scheme I, ±0.1% for LDD-scheme II).

The convergence is almost linear for both schemes, but only the LDD-scheme II is fast (see Fig. 9). The first scheme has a convergence rate of 0.999 and thus should not be used for applications including hysteresis, or at least needs to be improved by e.g. localizing the LDD parameter. Nevertheless, it has good convergence properties within

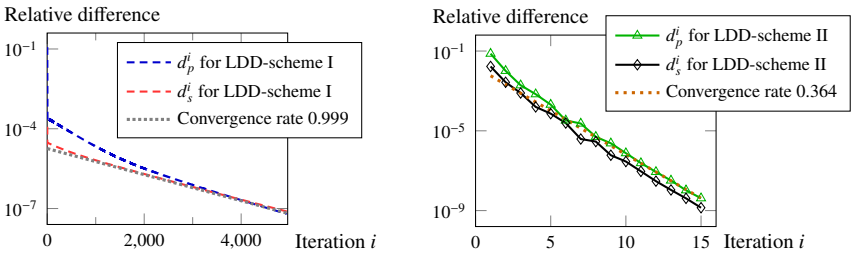

Figure 9: Both LDD-schemes converge almost linearly, but only the second one is fast in the last time step of the case with linear coefficient functions including hysteresis, for $\Delta t = 0.05$ and $\Delta x = 0.025$ (left) or $\Delta x = 0.0125$ (right). Plotted are the relative differences of pressure and saturation between consecutive iterations, together with the fitted convergence rates.

the first few iterations, and hence could be used as a preconditioner. The parameter dependence of the average number of iterations per time step is similar to the previous example. Only the LDD-scheme II has a clear optimal parameter set, whereas the first one shows almost no dependence on the domain decomposition parameter $\mathcal{L}_\Gamma$ (see Fig. 10). The lower bounds from our analysis are in this case $\mathcal{L}_p \geq 1/2$, $\mathcal{L}_T \geq 1/2$ and $\mathcal{L}_\Phi \geq 10^3$ for LDD-scheme I and $\mathcal{L}_p > 1$ for the second one. For the first scheme, this coincides very well with the observed optimum, while the bound for the second one is too restrictive for this application, but a good indicator of the optimal region.

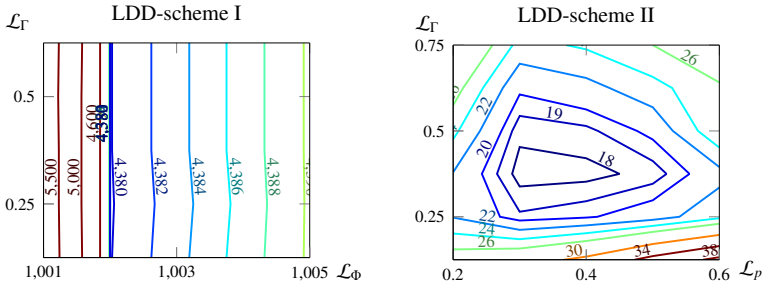

Figure 10: Parameter dependence of the average number of iterations per time step in the analytical case with linear coefficients including hysteresis. *Left:* $\delta = 5 \cdot 10^{-4}$, $\Delta t = 0.1$, $\Delta x = 0.05$. For simplicity $\mathcal{L}_p = \mathcal{L}_T = 0$. *Right:* $\delta = 10^{-9}$, $\Delta t = 0.1$, $\Delta x = 0.025$.

5.2. *Realistic Test Case*

This last subsection is dedicated to the study of a realistic problem including gravity. To this end, we choose a van-Genuchten-Mualem parameterization [67], with the relative permeabilities and the equilibrium capillary pressure given by

$$k_n(s) := \sqrt{1 - s_{\text{eff}}}\left(1 - s_{\text{eff}}^{1/m}\right)^{2m}, \qquad k_w(s) := \sqrt{s_{\text{eff}}}\left(1 - \left(1 - s_{\text{eff}}^{1/m}\right)^{m}\right)^2,$$
$$\tilde{p}_c(s, \mathbf{x}) := P\left(s_{\text{eff}}^{-1/m} - 1\right)^{1-m} - (\rho_n - \rho_w) g x_1, \quad s_{\text{eff}} := \tfrac{s - s_{\text{wr}}}{1 - s_{\text{wr}} - s_{\text{nr}}},$$

where the effective saturation s_{eff} accounts for the residual saturations s_{nr} and s_{wr}. The capillary pressure is scaled by a material-specific pressure P, and the retention exponent m determines the steepness of the S-shaped curve. Furthermore, we include dynamic capillarity and hysteresis by constant τ and γ within each subdomain. All the parameters are listed in Table 7 and inspired by the choices made in [68].

To obtain the non-dimensional equations (2.1)–(2.6), we chose the scaling parameters $L = 1$ m, $p^* = 2.5 \cdot 10^3$ Pa and $\tau^* = 1.5 \cdot 10^3$ Pa s and

$$\lambda_\alpha(s) = \tfrac{\tau^*}{\mu_\alpha} k_\alpha(s), \qquad K = \tfrac{\tilde{K}}{L^2}, \qquad p_c(s) = \tfrac{\tilde{p}_c(s)}{p^*}, \qquad \tau = \tfrac{\tilde{\tau}}{\tau^*}, \qquad \gamma = \tfrac{\tilde{\gamma}}{p^*}.$$

The domain $\Omega = (-0.5,\ 0.5) \times (0, 1)$ is decomposed into two subdomains at the interface $\Gamma = \{0\} \times (0, 1)$. We chose the final time $T = 400$ (real time 240 s) and initial conditions

Parameter	Symbol	Value		Unit
		Ω_1	Ω_2	
Porosity	ϕ	0.4	0.3	m^2
Absolute permeability	$\tilde{K}$	$3.0 \cdot 10^{-10}$	$5.0 \cdot 10^{-10}$	m^2
Material-specific pressure	P	$1.25 \cdot 10^3$	$1.0 \cdot 10^3$	Pa
Retention exponent	m	0.8	0.7	—
Residual saturation, non-wetting phase	s_{nr}	0.1	0.05	—
Residual saturation, wetting phase	s_{wr}	0.1	0.05	—
Typical redistribution parameter	$\tilde{\tau}$	$2.0 \cdot 10^3$	$1.5 \cdot 10^3$	Pa s
Hysteresis pressure parameter	$\tilde{\gamma}$	200	100	Pa
Density of the non-wetting phase	ρ_n	1.0		kg/m^3
Density of the wetting phase	ρ_w	$1.0 \cdot 10^3$		kg/m^3
Gravity (positive x-direction)	g	9.81		m/s^2
Viscosity of the non-wetting phase	μ_n	$2.0 \cdot 10^{-5}$		Pa s
Viscosity of the wetting phase	μ_w	$1.0 \cdot 10^{-3}$		Pa s

Table 7: Parameters of the van-Genuchten-Mualem model in the two subdomains for the realistic case.

with almost constant saturation given by

$$p_n^0(\mathbf{x}) = 0.75 - \tfrac{\rho_n g L}{p^*} x_1 = 0.75 - 0.003924 x_1, \qquad p_w^0(\mathbf{x}) = -\tfrac{\rho_w g L}{p^*} x_1 = -3.924 x_1,$$

$$s^0(\mathbf{x}) = p_c^{-1}\left(p_n^0(\mathbf{x}) - p_w^0(\mathbf{x})\right) \approx \begin{cases} 0.2431 & \text{if } x_1 < 0, \\ 0.2414 & \text{if } x_1 > 0. \end{cases}$$

The boundary conditions at $x_1 = \pm 0.5$ are of constant Dirichlet type, to mach the initial conditions, except for p_w at $x_1 = -0.5$ given by

$$p_w\big|_{x_1=-0.5} = 1.962 + \begin{cases} 0.015t & \text{if } t < 25, \\ 0.375 & \text{if } 25 \le t < 100, \\ 0.015 \cdot (125 - t) & \text{if } 100 \le t < 130, \\ -0.075 & \text{if } 125 \le t, \end{cases}$$

whereas the boundary conditions at $x_2 \in \{0, 1\}$ are of homogeneous Neumann type. By this choice, we simulate an imbibition and drainage cycle. The order of the spatial discretization was reduced to one, i.e. piece-wise linear and the tolerance for the LDD-schemes of 10^{-6}, since the solution is less smooth than in the analytical cases. In contrast to the manufactured examples above, we only studied the convergence of the LDD-schemes within the time steps. Therefore, the mesh width $\Delta x = 0.02$ and $\Delta t = 0.1$ are fixed. Note that the time step size here is about 100 times larger than in [68]. This might partially be a consequence of the different parameters and scaling, but also due to the L-scheme, whereas Schneider et al. used the Newton method.

The choice of the parameters and the results are shown in Table 8, and the obtained solutions for $\mathcal{L}_\Gamma = 0.5$ at time $t \in \{100, 200, 400\}$ are depicted in Fig. 11. The solutions of both methods are very similar, except for the small peaks near $x_1 = 0$. The latter seem to be an artifact of the numerical computation. Apart from that, the imbibition and drainage cycle can be clearly observed. Again, the huge parameter $\mathcal{L}_\Phi$ slows down the LDD-scheme I, whereas the second scheme has no such restriction. Although the average number of iterations per time step for the LDD-scheme I is smaller than in the

LDD-scheme	δ	$\mathcal{L}_p$	$\mathcal{L}_T$	$\mathcal{L}_\Phi$	$\mathcal{L}_\Gamma$	Avg.-Iter.
I	10^{-3}	1.0	1.3	40	0.5	868.7
I	10^{-3}	1.0	1.3	40	1.5	(706.1)
II		1.0	—	—	0.5	123.6
II		1.0	—	—	1.5	214.4

Table 8: Average number of iterations per time step for the realistic problem. The LDD-scheme I with $\mathcal{L}_\Gamma = 1.5$ does not converge at time $t = 158$ within 20000 iterations, such that the results in that case are only shown until then.

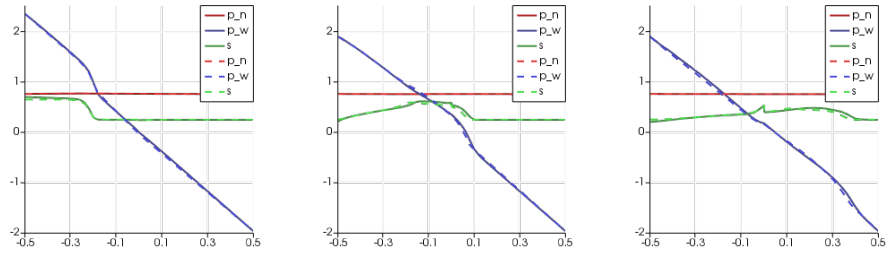

Figure 11: Numerical solution for the realistic case over x_1, at $x_2 = 0.5$ and the times $t = 100$ (left), $t = 200$ (center) and $t = 400$ (right). Dashed: LDD-scheme I. Solid: LDD-scheme II.

last example, the average number of iterations per time step for the LDD-scheme II is about eight times smaller. Note that both schemes are used with much smaller linearization parameters than those required by our analysis in Section 4, but give rise to better results than the required ones.

This time, we consider the convergence properties of the methods within one time step at the times $t = 150$ and $t = 250$. The first is shortly before the flow passes Γ, while the process switches at Γ from imbibition to drainage around the latter time. For both schemes, we observed convergence rates close to one (see Fig. 12), such that both schemes are slow and should be improved by e.g. localized linearization parameters. Nevertheless, the convergence is almost monotonous, except for the saturation in the second scheme, and the differences again decrease rapidly at the beginning. Furthermore, note that the LDD-scheme I does not converge at time $t = 158$ within 20000 iterations, when $\mathcal{L}_\Gamma = 1.5$. Since such problems would require different parameters for the two subdomains, which makes a proper choice even more challenging, we did not study the effect of varying parameters.

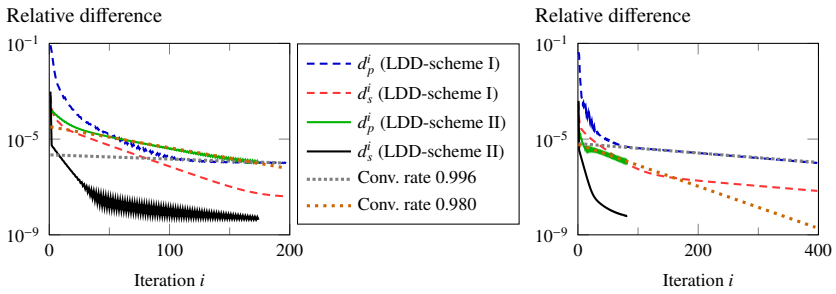

Figure 12: Both LDD-schemes converge very slow, and the first one rather linearly, at times $t = 150$ (left) and $t = 250$ (right) of the realistic case for $\Delta t = 0.1$ and $\Delta x = 0.025$ (left) or $\Delta x = 0.0125$ (right). Plotted are the relative differences of pressure and saturation between consecutive iterations, together with the fitted convergence rates.

6. Conclusion

Linearization and domain decomposition can be combined into one iteration, the LDD-scheme. For the considered non-equilibrium two-phase model, the proposed LDD-schemes lead to unique solutions, which converge towards the semi-discrete solutions of the model, as proved in Section 4. This convergence is global, i.e. independently of the initial guess, and requires only a mild restriction on the time step, independently of the spatial discretization. The inverted formulation for the capillary pressure in the LDD-scheme II avoids the necessary regularization for the original formulation in the LDD-scheme I.

The stability and robustness of both LDD-schemes were numerically verified for several spatially two-dimensional cases. The convergence rate can be improved significantly by a proper choice of the LDD-parameters. In particular, we pointed out the practical advantages of the second scheme, when hysteresis is present. While the analysis leads to good estimates for the linearization parameters, an estimate for the domain decomposition parameter is still an open problem.

The methods can be generalized, when the porosity ϕ and the dynamic capillarity coefficient τ are spatially variable, and when the hysteresis coefficient γ depends on the saturation s. Furthermore, the required regularity of the parameter functions may be relaxed to Hölder continuity as in [7, 8]. The degenerated cases $\lambda_w(0) = 0$ and $\lambda_n(1) = 0$ involve difficulties which need to be investigated in the future, as well as vanishing dynamic capillarity $\tau = 0$. Nonlinear interface conditions for entry-pressure models can be studied as soon as extensions for the case of dynamic and hysteretic capillarity are available.

The convergence properties of the schemes can be further improved by choosing the LDD-parameters depending on the position or the current solution. Finally, an a-posteriori error analysis can lead to estimates for efficient and adaptive stopping criteria, which would increase the performance even more.

References

[1] F. A. Radu, I. S. Pop, P. Knabner, Newton-type methods for the mixed finite element discretization of some degenerate parabolic equations, in: Numerical Mathematics and Advanced Applications ENUMATH 2005, Springer Berlin Heidelberg, 2006, pp. 1192–1200.

[2] I. S. Pop, F. A. Radu, P. Knabner, Mixed finite elements for the Richards' equation: Linearization procedure, J. Comput. Appl. Math. 168 (2004) 365–373.

[3] X. Cao, K. Mitra, Error estimates for a mixed finite element discretization of a two-phase porous media flow model with dynamic capillarity, J. Comput. Appl. Math. 353 (2019) 164–178.

[4] F. List, F. A. Radu, A study on iterative methods for solving Richards' equation, Comput. Geosci. 20 (2016) 341–353.

[5] S. Karpinski, I. S. Pop, F. A. Radu, Analysis of a linearization scheme for an interior penalty discontinuous Galerkin method for two-phase flow in porous media with dynamic capillarity effects, Int. J. Numer. Meth. Engng. 112 (2017) 553–577.

[6] X. Cao, S. F. Nemadjieu, I. S. Pop, Convergence of an MPFA finite volume scheme for a two-phase porous media flow model with dynamic capillarity, IMA J. Numer. Anal. 39 (2018) 512–544.

[7] F. A. Radu, K. Kumar, J. M. Nordbotten, I. S. Pop, A robust, mass conservative scheme for two-phase flow in porous media including Hölder continuous nonlinearities, IMA J. Numer. Anal. 38 (2017) 884–920.

[8] J. W. Both, K. Kumar, J. M. Nordbotten, I. S. Pop, F. A. Radu, Iterative linearization schemes for doubly degenerate parabolic equations, in: Numerical Mathematics and Advanced Applications ENUMATH 2017, Springer International Publishing, 2019, pp. 49–63.

[9] H. A. Schwarz, Über einen Grenzübergang durch alternierendes Verfahren, Vierteljahrsschrift der Naturforschenden Gesellschaft in Zürich 15 (1870) 272–286.

[10] P.-L. Lions, On the Schwarz alternating method. I, in: First International Symposium on Domain Decomposition Methods for Partial Differential Equations, 1988, pp. 1–42.

[11] P.-L. Lions, On the Schwarz alternating method III: A variant for nonoverlapping subdomains, in: Third International Symposium on Domain Decomposition Methods for Partial Dierential Equations, SIAM, 1990, pp. 202–223.

[12] M. J. Gander, L. Halpern, F. Nataf, Optimal Schwarz waveform relaxation for the one dimensional wave equation, SIAM J. Numer. Anal. 41 (2003) 1643–1681.

[13] M. J. Gander, C. Rohde, Overlapping Schwarz waveform relaxation for convection-dominated nonlinear conservation laws, SIAM J. Sci. Comput. 27 (2005) 415–439.

[14] M. J. Gander, L. Halpern, Optimized Schwarz waveform relaxation methods for advection reaction diffusion problems, SIAM J. Numer. Anal. 45 (2007) 666–697.

[15] F. Caetano, M. J. Gander, L. Halpern, J. Szeftel, Schwarz waveform relaxation algorithms for semilinear reaction-diffusion equations, NHM 5 (2010) 487–505.

[16] M. J. Gander, O. Dubois, Optimized Schwarz methods for a diffusion problem with discontinuous coefficient, Numer. Algor. 69 (2015) 109–144.

[17] S. B. Lunowa, C. Rohde, M. J. Gander, Non-overlapping Schwarz waveform-relaxation for quasi-linear convection-diffusion equations, in preparation (2020).

[18] D.-G. Calugaru, D. Tromeur-Dervout, Non-overlapping DDMs to solve flow in heterogeneous porous media, in: Domain Decomposition Methods in Science and Engineering, Springer-Verlag, 2005, pp. 529–536.

[19] H. Berninger, R. Kornhuber, O. Sander, Convergence behaviour of Dirichlet–Neumann and Robin methods for a nonlinear transmission problem, in: Domain decomposition methods in science and engineering XIX, Springer, 2011, pp. 87–98.

[20] E. Ahmed, S. A. Hassan, C. Japhet, M. Kern, M. Vohralík, A posteriori error estimates and stopping criteria for space-time domain decomposition for two-phase flow between different rock types, SMAI J. Comput. Math. 5 (2019) 195–227.

[21] E. Ahmed, Splitting-based domain decomposition methods for two-phase flow with different rock types, Adv. Water Resour. 134 (2019) 103431.

[22] D. Seus, K. Mitra, I. S. Pop, F. A. Radu, C. Rohde, A linear domain decomposition method for partially saturated flow in porous media, Comput. Methods Appl. Mech. Eng. 333 (2018) 331–355.

[23] D. Seus, F. A. Radu, C. Rohde, A linear domain decomposition method for two-phase flow in porous media, in: Numerical Mathematics and Advanced Applications ENUMATH 2017, Springer International Publishing, 2019, pp. 603–614.

[24] S. B. Lunowa, Linearization and domain decomposition methods for two-phase flow in porous media, Master's thesis, Eindhoven University of Technology (2018).
URL https://research.tue.nl/en/studentTheses/linearization-and-domain-decomposition-methods

[25] S. B. Lunowa, I. S. Pop, B. Koren, A linear domain decomposition method for non-equilibrium two-phase flow models, UHasselt Preprint UP-19-14 (2019).
URL https://www.uhasselt.be/Documents/CMAT/Preprints/2019/UP1914.pdf

[26] C. J. van Duijn, J. Molenaar, M. J. de Neef, The effect of capillary forces on immiscible two-phase flow in heterogeneous porous media, Transp. Porous Med. 21 (1995) 71–93.

[27] F. Buzzi, M. Lenzinger, B. Schweizer, Interface conditions for degenerate two-phase flow equations in one space dimension, Analysis 29 (2009) 299–316.

[28] C. Cancès, M. Pierre, An existence result for multidimensional immiscible two-phase flows with discontinuous capillary pressure field, SIAM J. Math. Anal. 44 (2012) 966–992.

[29] C. J. van Duijn, X. Cao, I. S. Pop, Two-phase flow in porous media: Dynamic capillarity and heterogeneous media, Transp. Porous Med. 114 (2016) 283–308.

[30] D. A. DiCarlo, Experimental measurements of saturation overshoot on infiltration, Water Resour. Res. 40 (2004).

[31] S. Bottero, S. M. Hassanizadeh, P. J. Kleingeld, T. J. Heimovaara, Nonequilibrium capillarity effects in two-phase flow through porous media at different scales, Water Resour. Res. 47 (2011).

[32] L. Zhuang, S. M. Hassanizadeh, C.-Z. Qin, A. de Waal, Experimental investigation of hysteretic dynamic capillarity effect in unsaturated flow, Water Resour. Res. 53 (2017) 9078–9088.

[33] L. Zhuang, S. M. Hassanizadeh, C. J. van Duijn, S. Zimmermann, I. Zizina, R. Helmig, Experimental and numerical studies of saturation overshoot during infiltration into a dry soil, Vadose Zone Journal 18 (2019) 180167.

[34] J. C. Parker, R. J. Lenhard, A model for hysteretic constitutive relations governing multiphase flow: 1. Saturation-pressure relations, Water Resour. Res. 23 (1987) 2187–2196.

[35] R. Helmig, A. Weiss, B. I. Wohlmuth, Dynamic capillary effects in heterogeneous porous media, Comput. Geosci. 11 (2007) 261–274.

[36] J. Niessner, S. M. Hassanizadeh, A model for two-phase flow in porous media including fluid-fluid interfacial area, Water Resour. Res. 44 (2008).

[37] R. Helmig, A. Weiss, B. I. Wohlmuth, Variational inequalities for modeling flow in heterogeneous porous media with entry pressure, Comput. Geosci. 13 (2009) 373–389.

[38] I. S. Pop, C. J. van Duijn, J. Niessner, S. M. Hassanizadeh, Horizontal redistribution of fluids in a porous medium: The role of interfacial area in modeling hysteresis, Adv. Water Resour. 32 (2009) 383–390.

[39] A. Papafotiou, H. Sheta, R. Helmig, Numerical modeling of two-phase hysteresis combined with an interface condition for heterogeneous porous media, Comput. Geosci. 14 (2009) 273–287.

[40] C. J. van Duijn, K. Mitra, Hysteresis and horizontal redistribution in porous media, Transp. Porous Med. 122 (2018) 375–399.

[41] S. M. Hassanizadeh, W. G. Gray, Thermodynamic basis of capillary pressure in porous media, Water Resour. Res. 29 (1993) 3389–3405.

[42] A. Y. Beliaev, S. M. Hassanizadeh, A theoretical model of hysteresis and dynamic effects in the capillary relation for two-phase flow in porous media, Transp. Porous Med. 43 (2001) 487–510.

[43] B. Schweizer, Instability of gravity wetting fronts for Richards equations with hysteresis, Interfaces Free Bound. 14 (2012) 37–64.

[44] R. Hilfer, R. Steinle, Saturation overshoot and hysteresis for twophase flow in porous media, Eur. Phys. J. Spec. Top. 223 (2014) 2323–2338.

[45] A. Rätz, B. Schweizer, Hysteresis models and gravity fingering in porous media, Z. angew. Math. Mech. 94 (2014) 645–654.

[46] K. Mitra, C. J. van Duijn, Wetting fronts in unsaturated porous media: The combined case of hysteresis and dynamic capillary pressure, Nonlinear Anal. Real World Appl. 50 (2019) 316–341.

[47] B. Schweizer, The Richards equation with hysteresis and degenerate capillary pressure, J. Differ. Equ. 252 (2012) 5594–5612.

[48] J. Koch, A. Rätz, B. Schweizer, Two-phase flow equations with a dynamic capillary pressure, Eur. J. Appl. Math. 24 (2012) 49–75.

[49] X. Cao, I. S. Pop, Two-phase porous media flows with dynamic capillary effects and hysteresis: Uniqueness of weak solutions, Comput. Math. Appl. 69 (2015) 688–695.

[50] A. Lamacz, A. Rätz, B. Schweizer, A well-posed hysteresis model for flows in porous media and applications to fingering effects, Advances in Mathematical Sciences and Applications 21 (2011) 33–64.

[51] L. A. Richards, Capillary conduction of liquids through porous mediums, Physics 1 (1931) 318–333.

[52] H. Berninger, S. Loisel, O. Sander, The 2-Lagrange multiplier method applied to nonlinear transmission problems for the Richards equation in heterogeneous soil with cross points, SIAM J. Sci. Comput. 36 (2014) A2166–A2198.

[53] B. Schweizer, Regularization of outflow problems in unsaturated porous media with dry regions, J. Differ. Equ. 237 (2007) 278–306.

[54] A. Mikelić, A global existence result for the equations describing unsaturated flow in porous media with dynamic capillary pressure, J. Differ. Equ. 248 (2010) 1561–1577.

[55] X. Cao, I. S. Pop, Degenerate two-phase porous media flow model with dynamic capillarity, J. Differ. Equ. 260 (2016) 2418–2456.

[56] J.-P. Milišić, The unsaturated flow in porous media with dynamic capillary pressure, J. Differ. Equ. 264 (2018) 5629–5658.

[57] X. Cao, I. S. Pop, Uniqueness of weak solutions for a pseudo-parabolic equation modeling two phase flow in porous media, Appl. Math. Lett. 46 (2015) 25–30.

[58] F. Brezzi, M. Fortin, Mixed and Hybrid Finite Element Methods, Vol. 15 of Springer Series In Computational Mathematics, Springer New York, 1991.

[59] R. Eymard, C. Guichard, R. Herbin, R. Masson, Gradient schemes for two-phase flow in heterogeneous porous media and Richards equation, Z. angew. Math. Mech. 94 (2013) 560–585.

[60] Q. Deng, An analysis for a nonoverlapping domain decomposition iterative procedure, SIAM J. Sci. Comput. 18 (1997) 1517–1525.

[61] A. Ern, I. Mozolevski, L. Schuh, Discontinuous galerkin approximation of two-phase flows in heterogeneous porous media with discontinuous capillary pressures, Comput. Methods Appl. Mech. Eng. 199 (2010) 1491–1501.

[62] G. Enchéry, R. Eymard, A. Michel, Numerical approximation of a two-phase flow problem in a porous medium with discontinuous capillary forces, SIAM J. Numer. Anal. 43 (2006) 2402–2422.

[63] K. Brenner, C. Cancès, D. Hilhorst, Finite volume approximation for an immiscible two-phase flow in porous media with discontinuous capillary pressure, Comput. Geosci. 17 (2013) 573–597.

[64] K. Bouadjila, A. Mokrane, S. A. Saad, M. Saad, Numerical analysis of a finite volume scheme for two incompressible phase flow with dynamic capillary pressure, Comput. Math. Appl. 75 (2018) 3614–3631.

[65] J. Droniou, R. Eymard, High-order mass-lumped schemes for nonlinear degenerate elliptic equations, SIAM J. Numer. Anal. 58 (2020) 153–188.

[66] G. Alzetta, et al., The deal.II library, version 9.0, J. Numer. Math. 26 (2018) 173–183.

[67] M. T. van Genuchten, A closed-form equation for predicting the hydraulic conductivity of unsaturated soils, Soil Sci. Soc. Am. J. 44 (1980) 892.

[68] M. Schneider, T. Köppl, R. Helmig, R. Steinle, R. Hilfer, Stable propagation of saturation overshoots for two-phase flow in porous media, Transp. Porous Med. 121 (2017) 621–641.

UHasselt Computational Mathematics Preprint Series

2020

UP-20-03 *S.B. Lunowa, I.S. Pop, and B. Koren*, **Linearization and Domain Decomposition Methods for Two-Phase Flow in Porous Media Involving Dynamic Capillarity and Hysteresis**, 2020

UP-20-02 *M. Bastidas, C. Bringedal, and I.S. Pop*, **Numerical simulation of a phase-field model for reactive transport in porous media**, 2020

UP-20-01 *S. Sharmin, C. Bringedal, and I.S. Pop*, **Upscaled models for two-phase flow in porous media with evolving interfaces at the pore scale**, 2020

2019

UP-19-17 *C. Bringedal*, **A conservative phase-field model for reactive transport**, 2019

UP-19-16 *D. Landa-Marbán, G. Bødtker, B.F. Vik, P. Pettersson, I.S. Pop, K. Kumar, F.A. Radu*, **Mathematical Modeling, Laboratory Experiments, and Sensitivity Analysis of Bioplug Technology at Darcy Scale**, 2019

UP-19-15 *D. Illiano, I.S. Pop, F.A. Radu*, **An efficient numerical scheme for fully coupled flow and reactive transport in variably saturated porous media including dynamic capillary effects**, 2019

UP-19-14 *S.B. Lunowa, I.S. Pop, and B. Koren*, **A Linear Domain Decomposition Method for Non-Equilibrium Two-Phase Flow Models**, 2019

UP-19-13 *C. Engwer, I.S. Pop, T. Wick*, **Dynamic and weighted stabilizations of the L-scheme applied to a phase-field model for fracture propagation**, 2019

UP-19-12 *M. Gahn*, **Singular limit for quasi-linear diffusive transport through a thin heterogeneous layer**, 2019

UP-19-11 *M. Gahn, W. Jäger, M. Neuss-Radu*, **Correctors and error estimates for reaction-diffusion processes through thin heterogeneous layers in case of homogenized equations with interface diffusion**, 2019

UP-19-10 *V. Kučera, M. Lukáčová-Medvidová, S. Noelle, J. Schütz,*, **Asymptotic properties of a class of linearly implicit schemes for weakly compressible Euler equations**, 2019

UP-19-09 *D. Seal, J. Schütz*, **An asymptotic preserving semi-implicit multiderivative solver**, 2019

UP-19-08 *H. Hajibeygi, M. Bastidas Olivares, M. HosseiniMehr, I.S. Pop, M.F. Wheeler*, **A benchmark study of the multiscale and homogenization methods for fully implicit multiphase ow simulations with adaptive dynamic mesh (ADM)**, 2019

UP-19-07 *J.W. Both, I.S. Pop, I. Yotov*, **Global existence of a weak solution to unsaturated poroelasticity**, 2019

UP-19-06 *K. Mitra, T. Köppl, I.S. Pop, C.J. van Duijn, R. Helmig*, **Fronts in two-phase porous flow problems: effects of hysteresis and dynamic capillarity**, 2019

UP-19-05 *D. Illiano, I.S. Pop, F.A. Radu*, **Iterative schemes for surfactant transport in porous media**, 2019

UP-19-04 *M. Bastidas, C. Bringedal, I.S. Pop, F.A. Radu*, **Adaptive numerical homogenization of nonlinear diffusion problems**, 2019

UP-19-03 *K. Kumar, F. List, I.S. Pop, F.A. Radu*, **Formal upscaling and numerical validation of fractured flow models for Richards' equation**, 2019

UP-19-02 *M.A. Endo Kokubun, A. Muntean, F.A. Radu, K. Kumar, I.S. Pop, E. Keilegavlen, K. Spildo*, **A pore-scale study of transport of inertial particles by water in porous media**, 2019

UP-19-01 *C. Bringedal, L. von Wolff, and I.S. Pop*, **Phase field modeling of precipitation and dissolution processes in porous media: Upscaling and numerical experiments**, 2019